Study of the Self-assembly of a Nonionic Surfactant at Aqueous-Liquid Crystal Interfaces

Sukanya Dutta

A dissertation submitted for the partial fulfilment of MS degree in Science

Indian Institute of Science Education and Research Mohali
April 2021

Certificate of Examination

This is to certify that the dissertation titled **"Study of the Self-assembly of a Nonionic Surfactant at Aqueous-Liquid crystal Interfaces''** submitted by **Ms. Sukanya Dutta** (Reg. No. MP18025) for the partial fulfilment of MS degree programme of the Institute, has been examined by the thesis committee duly appointed by the Institute. The committee finds the work done by the candidate satisfactory and recommends that the report be accepted.

Dr. Subhabrata Maiti Dr. Raj Kumar Roy Dr. Santanu K.Pal

(Supervisor)

Dated: April 30th, 2021

Declaration

The work presented in this dissertation has been carried out by me under the guidance of Dr. Santanu K. Pal at the Indian Institute of Science Education and Research Mohali.

This work has not been submitted in part or in full for a degree, a diploma, or a fellowship to any other university or institute. Whenever contributions of others are involved, every effort is made to indicate this clearly, with due acknowledgement of collaborative research and discussions. This thesis is a bonafide record of original work done by me and all sources listedwithin have been detailed in the bibliography.

Sukanya Dutta (Candidate)

Dated: April 30th, 2021

In my capacity as the supervisor of the candidate's project work, I certify that the above statements by the candidate are true to the best of my knowledge.

Dr. Santanu K. Pal

(Supervisor)

Acknowledgement

First and foremost, I would like to thank my supervisor **Dr. Santanu K. Pal** for his constant guidance and support throughout the journey. I would also like to thank **Ms. Ipsita Pani** for her hands on guidance throughout the project. This would not have been possible if it were not for their helpful discussions and directions that resulted in successful completion of the project.

I thank **Dr. Subhabrata Maiti** and **Dr. Raj Kumar Roy**, members of my doctoral committee, for timely and fruitful discussions throughout my project work. I am grateful to all the faculties of IISER for their teaching, encouragement and helpful advice.

I would also like to acknowledge our collaborator **Mr. Yogendra Nailwal** from our lab for synthesizing the nonionic surfactant (Surf-LTE), around which my project revolves.

I would also like to thank all the members of my lab especially **Vidhika Di**, **Joydip Da**, **Tarang Di** and **Ritobrata** for helping me find my way whenever I seemed to hit a dead end during my project. I would also like to thank my closest friends **Jnanajyoti** and **Sumaiya** for constantly motivating me throughout this journey.

I am thankful to **IISER Mohali** for providing me with fellowship for 3 years and also for all the research facilities and instrumentation available.

I would also like to thank **IISER Mohali Library** for all the services they provided me with throughout this journey.

Last but not the least, I would like to acknowledge the support and love of my family members (including my cats) back at home. Especially my Father and Grandfather have played the biggest role in making me understand the importance of having patience, tenacity and courage in every possible situation life may bring. Without them I would not be able to find my way throughout the entire course of this journey.

Thank you all!

Sukanya Dutta

List of Figures

List of Tables

List of Abbreviations

LC	Liquid Crystal
5CB	4-Cyano-4'-pentylbiphenyl
Surf-LTE	Tetra (ethylene glycol) mono-n-dodecanoate
LA	Lauric acid
DPH	1,6-diphenyl-1,3,5-hexatriene
NR	Nile Red
CMC	Critical Micelle Concentration
DMOAP	N,N-dimethyl-N-octadecyl-3-aminopropyltrimethoxysilyl chloride
PBS	Phosphate-buffered saline
BSA	Bovine serum albumin
POM	Polarized Optical Microscopy
TEM grid	Transmission Electron Microscopy grid

Abstract

Nematic liquid crystals (LCs) are anisotropic materials, whose long orientational order and high fluidity help to direct molecular assembly and amplify interfacial events into easily observable optical signals. Owing to the environment-sensitive fast response of LCs, they have been substantially studied to understand different complex biomolecular events at the interface. The self-assembly of surfactants, polymers, and other amphiphilic molecules at the nematic LC-aqueous interface, as well as the subsequent optical and orientational transitions in LC, have been extensively studied over the past few decades. In our project, we are trying to investigate various interfacial phenomena at aqueous-LC interfaces, using the polarised optical microscope (POM), that triggers orientational ordering transition of liquid crystal in the presence of the self-assembly of a nonionic surfactant tetra (ethylene glycol) mono-n-dodecanoate (Surf-LTE) and its cleaved fragments to understand the underlying mechanisms of such interactions. Keeping the goal of sustainable chemistry in mind, we are working with an eco-friendly bio-degradable nonionic surfactant system (Surf-LTE) that was synthesized in our lab. We have determined the critical micelle concentration (CMC) of Surf-LTE using the fluorescence probe method (DPH assay). Next, we have performed a set of polarized optical microscopy (POM) experiments and observed that Surf-LTE could spontaneously assemble at aqueous-LC interfaces to induce homeotropic orientations of the LC mesogens. The stability of such anchoring transition was also checked by varying the pH and salt concentration of the aqueous medium. In presence of a targeted stimulus (enzymes such as lipase) cleavage of the ester bond triggered a surface-driven ordering transition to a planar alignment of LC mesogens leading to a macroscopic bright optical signal. The optical response of precleaved moieties and cleaved fragments at the aqueous-LC interfaces was also found to be similar.

The results of our study so far exhibit a straightforward and broad approach to the rational design of nonionic surfactant systems that can be used to program stimuli-responsiveness into nematic LC-aqueous interfaces. The results provide an easy readout of interfacial events over time without the use of complex instruments and it is also label-free. The results of this study can have further applications in drug delivery thus enhancing its potential in the advancement of therapeutics.

Table of Contents

Chapter 1

Introduction

1.1 Liquid Crystals

The two most common condensed phases of matter are solids and liquids. The major difference between them lies in their order; while solids possess both positional and orientational order, liquids possess none. Liquid crystals (LCs) are an intermediate state of matter that shares the properties of both solids and liquids.[1] LCs possess many physical attributes similar to liquids, major of which is mobility; at the same time, LCs also have anisotropic physical properties (such as optical, electrical, magnetic anisotropy, etc.) similar to solids due to the presence of order. Thus, the LCs are also called mesophases and the molecules exhibiting such properties are termed mesogens.

Temperature is a measure of randomness. With increasing temperature, the random molecular motions increase and the attractive intermolecular forces decrease thus resulting in a phase transition.[2]

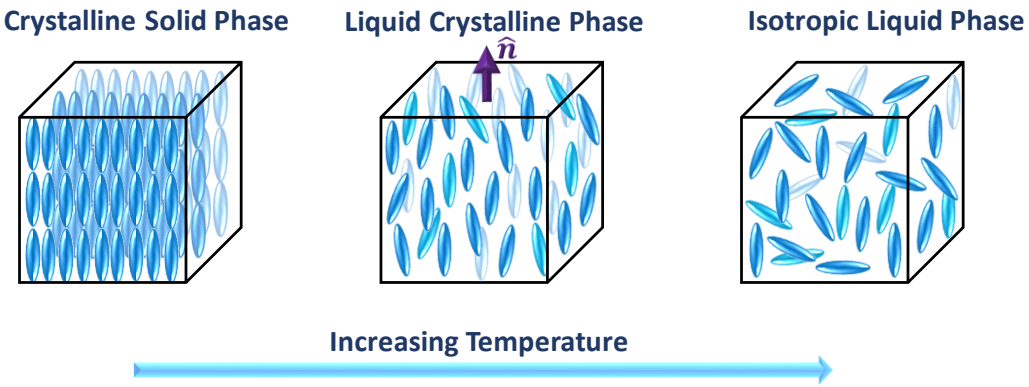

Figure 1.1. Cartoon illustration of the temperature dependent phases of a LC material. Redrawn from reference [9].

The liquid crystalline phase was observed in 1888 by Friedrich Reinitzer, an Austrian botanist and chemist.[3] He discovered that cholesterol benzoate had two distinct melting points. A turbid liquid phase was observed at 145.5ºC which changed into a clear liquid state at 178.5ºC upon further heating. He then discussed his findings with the German physicist Otto Lehmann. Lehman carried out further optical characterization studies of the turbid phase under a polarizing microscope. He concluded that the turbid phase exhibited properties of both solids and liquids and thus coined the term 'Liquid Crystal'.[4]

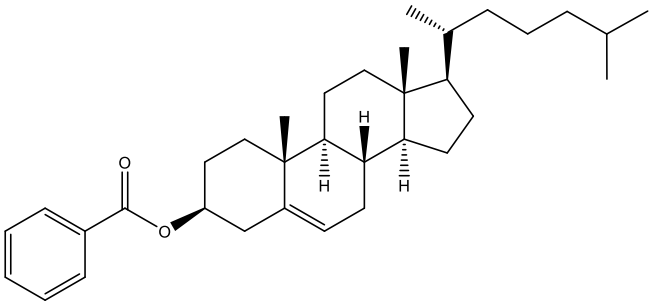

Figure 1.2. Chemical structure of cholesterol benzoate.

1.1.1. Classification of LCs

Thermotropic and lyotropic LCs are the two major types of LCs that can be found in nature. For thermotropic LCs, the mesophase formation is dependent on temperature, while in the case of lyotropic LCs the mesophase formation is dependent on the choice of solvent and concentration. Based on the shape of the mesogen molecules, the thermotropic LC can be further classified into three categories, which are calamitic LC (prolate, rod-shaped mesogens), discotic LC (oblate, disc-shaped mesogens) and bent-shape LC (nonlinear, bent shaped mesogens). The detailed classification is shown below in the chart.[5]

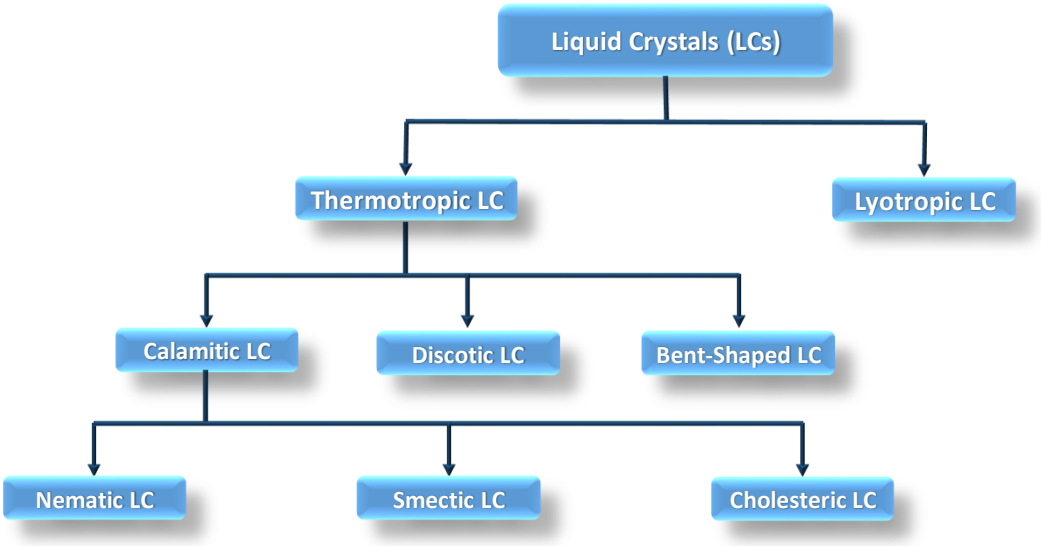

Figure 1.3. Classification of LCs.

In this thesis, we have worked with 5CB, which is a thermotropic nematic LC. It exhibits the LC phase near room temperature (24ºC-35ºC).

1.1.2. Nematic LCs

The nematic phase is the least ordered and simplest LC phase, which belongs to the class of thermotropic LCs. The terminology nematic comes from the Greek prefix 'Nematos', which primarily means thread-like. This is due to the observed optical textures of this phase under crossed polars. Both calamitic and discotic LCs can generate nematic LC phase, but they are different from each other and thus immiscible. The nematic mesogens possess a long-range orientational order but no long-range positional order. Nematic mesogens can exhibit uniaxial or biaxial symmetry.[6] 5CB is an example of prolate-like mesogen and exhibits the simpler uniaxial symmetry. Here, the mesogens tend to align themselves in a preferred orientation along a single director, which is a vector of unit length and is denoted by $\hat{n}$. The mesogens can freely rotate along the long axes without any preferred arrangements along the two ends of the mesogens (which are not chemically equivalent). Thus $\hat{n}$ and $-\hat{n}$ are equivalent.[7]

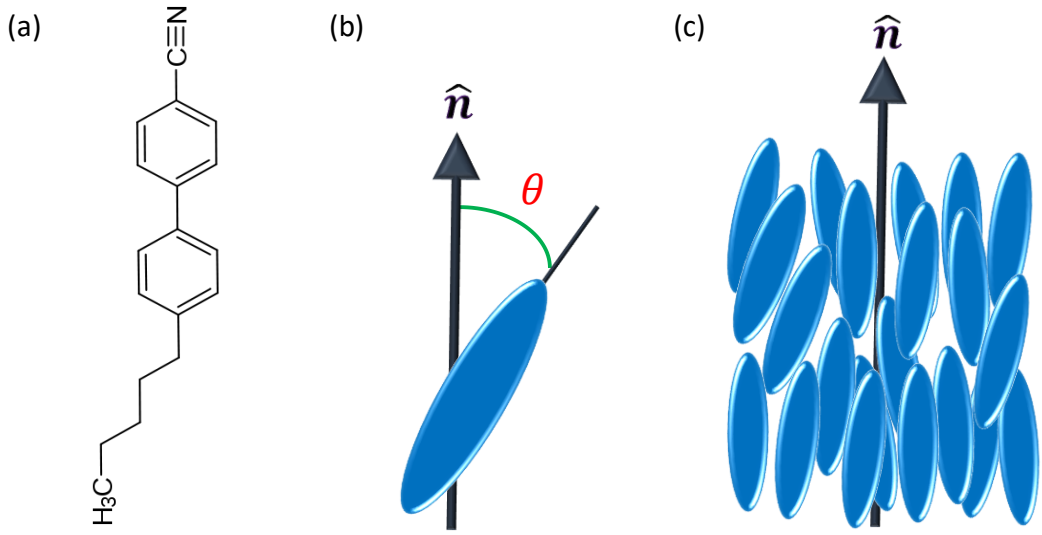

Figure 1.4. (a) Chemical structure of 5CB. (b) The average deviation angle (θ) formed between the mesogen axes with director is shown. (c) Schematic of a nematic mesophase depicting long-range orientational ordering. Redrawn from reference [9].

While director ($\hat{n}$) defines the average orientation of the mesogens, the degree of order within the phase is described by the order parameter S, which is defined as

$$S = \frac{1}{2}\langle 3\cos^2\theta - 1\rangle \qquad (1)$$

Here, θ represents the average deviation angle formed between the mesogen axes with the director.

$S = 0$; For the case of isotropic liquid phase, where all molecules are in statistical distribution

$S = 1$; For the case of crystalline solids, where all the molecules are aligned parallel to the director

$0.7 > S > 0.3$; For the case of nematic phases of LCs

The LC mesogens tend to orient themselves in a certain direction to minimize the surface free energy when confined within a surface. This certain orientation is denoted by the nematic director, termed as 'easy axis'. Any external disturbance at the surface causes the average orientation of mesogens to deviate from the easy axis. The average new orientation of the mesogens is denoted by a surface director.[8] The amount of energy required for this deviation is known as 'Surface Anchoring Energy' (W_a) and can be described using the following equation;

$$S = S_0 + \frac{1}{2}\langle W_a \sin^2(\theta_s - \theta_e)\rangle \quad (2)$$

Here,

S = Total interfacial free energy

S_0 = Interfacial free energy independent of the orientation of the mesogens

W_a = Surface anchoring energy

θ_s = Orientation of surface director

θ_e = Orientation of easy axis

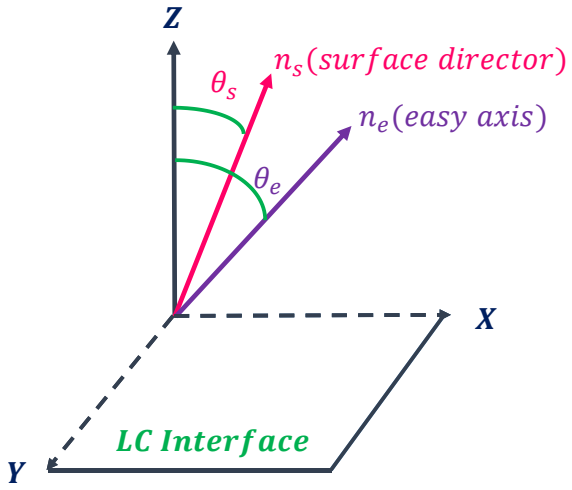

Figure 1.5. Orientation of nematic LC at the interface. Redrawn from reference [9].

For the nematic LC phase, the value of S lies in the range of 10^{-3} to 10^{-2} mJ/m^2. Due to such low interfacial energy, nematic LCs have been extensively used in the design of stimuli-responsive interfaces for applications in biosensing.

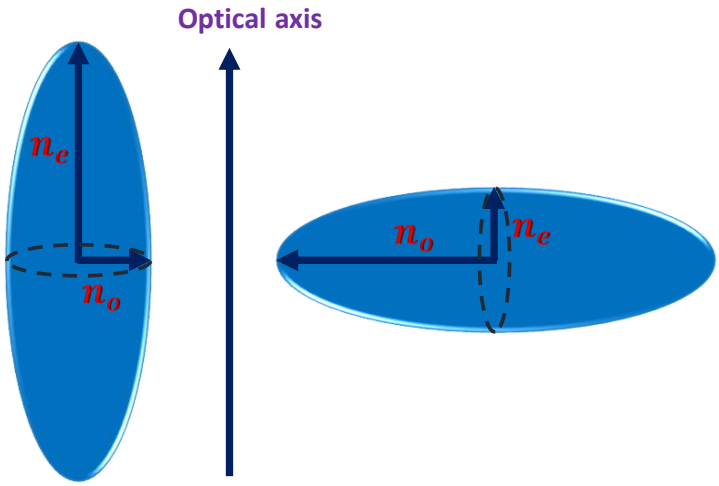

Figure 1.6. Cartoon illustration of mesogens showing optically positive (left) and optically negative (right) behavior. Redrawn from reference [53].

Another interesting property of the LCs is birefringence, which also acts as a major contributing factor in LC-based biosensing applications.[9] The mesophase of a uniaxial nematic LC exhibits optical anisotropy or birefringence. This phase has two principal refractive indices, which are as follows;

- Ordinary index (n_o): The refractive index is perpendicular to the optical axis.
- Extra-ordinary index (n_e): The refractive index is parallel with the optical axis.

  Birefringence is defined as

$$\Delta \boldsymbol{n} = \boldsymbol{n_e} - \boldsymbol{n_o} \qquad \textbf{(3)}$$

  For $n_e > n_o$; the material is known as optically positive.

  Similarly, for $n_o > n_e$; the material is known as optically negative.

Due to this optical anisotropy property, when light passes through the LC medium, the velocity of light differs from each other along the perpendicular and parallel directions with respect to the optical axis. Thus we observe different colored textures of the LC medium under crossed polars.

1.1.3. Principle of LC-based Biosensing

A biosensor detects substances that are either hazardous or essential to life by converting any biological signal to an electrical signal. An ideal biosensor should be simple (any layman can easily understand without the help of an expert), quick, highly sensitive, quantitative and inexpensive.[10] Abbott et al. first introduced LCs into the field of biosensing as it exhibits many properties that make it a perfect candidate for being an ideal biosensor.[11]

The combination of various physical properties such as optical anisotropy (birefringence), surface anchoring energy, and elasticity makes it a perfect tool for optical sensing. In the past few decades with the help of extensive studies, LCs have emerged as a powerful tool in the field of biosensing. The interaction between the LC mesogens at the interface with different analytes under special environmental conditions lead to a change in the orientational order of the LC and the signal is transmitted through bulk (up to a hundred micrometers) through co-operative interactions resulting in a change in the optical appearance under crossed polars. Based on the orientational and optical properties of the LCs, both lyotropic (water-based) and thermotropic (oil-based) LCs have shown promising results as biosensors. As most thermotropic LCs are immiscible with water, they interact with various analytes through distinct LC-water interfaces. Amongst the two major thermotropic LC-based biosensor formats, we have worked with the planar freestanding liquid crystal films throughout this thesis. The design of this type of sensor is shown in figure 1.7.

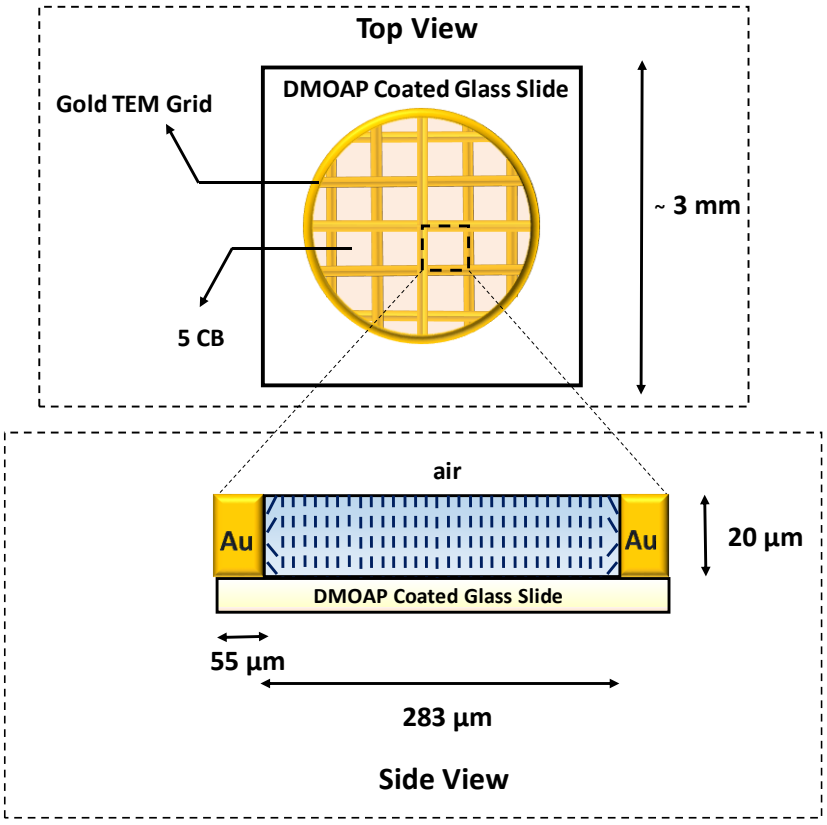

Figure 1.7. Cartoon illustration of the experimental set up for creating LC-aqueous interface. Redrawn from reference [9].

Here, LC is suspended in a gold TEM grid (20 μm thick). The grid is supported on a glass substrate that has been chemically modified with a hydrophobic substance (silanes such as DMOAP, OTS). This coating aligns the LC mesogens perpendicular to the surface, which is known as homeotropic or vertical alignment. When the top surface of LC is in contact with air, again homeotropic anchoring is promoted, thus leading to a uniform vertical alignment of the director throughout the bulk and results in an optical dark appearance under the crossed polars. When the supported LC film is submerged in an aqueous medium to make a uniform aqueous LC interface, interactions with water molecules align the LC mesogens parallel to the substrate, which is known as the planar alignment. Thus a hybrid configuration is generated throughout the bulk and results in a bright appearance under the crossed polars. At the addition of amphiphilic molecules such as surfactants in the bulk medium, a dark appearance is again observed, which is consistent with the Homeotropic alignment of the LC.[12] The changes in the optical appearance due to changes in orientational order of LC can be easily visualized using a polarised optical microscope (POM). The working principle of POM is described in the following figures (1.8 & 1.9).

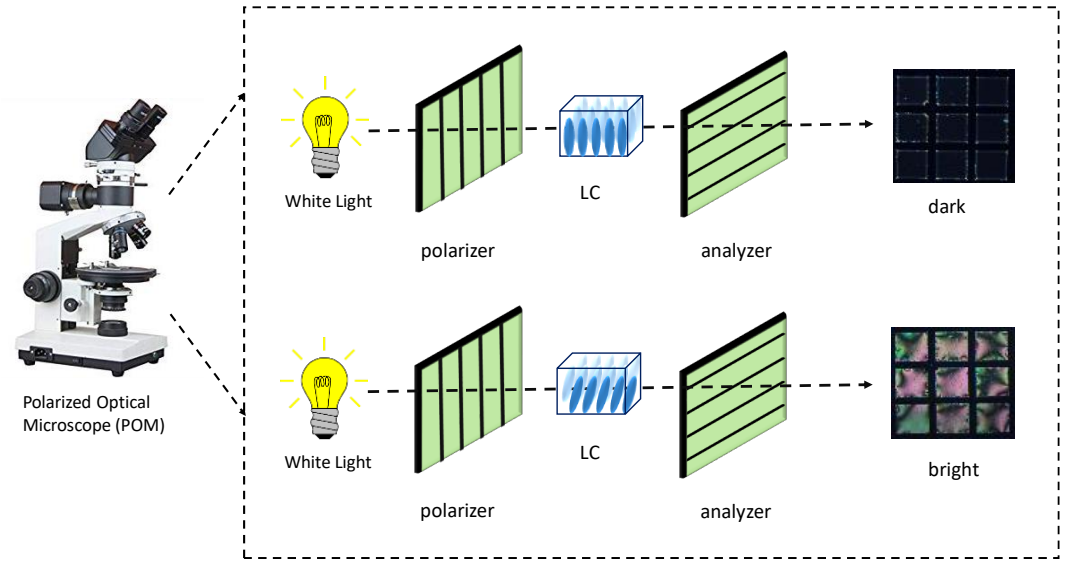

Figure 1.8. Cartoon representation of the working principle of a polarized optical microscope equipped with crossed polarizers. Change in the optical signal depends on the anchoring transition of LCs.

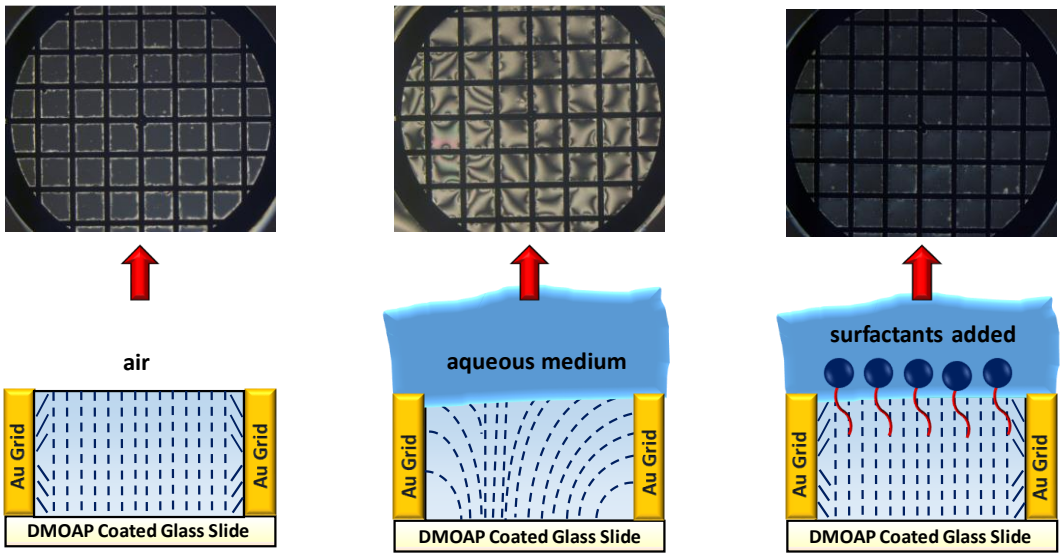

Figure 1.9. Rrepresentative POM images and corresponding cartoon illustrations of the LC ordering in contact with air, water, and surfactants in the aqueous phase. Redrawn from reference [54].

Thus LC-based biosensing provides a label-free detection method with very low detection limits (up to nM), high sensitivity, and easy optical readout without the requirement for any complex instrumentation.

1.2. Surfactants

Surfactant (abbreviated from the term *surface active agent*) is a substance that reduces the natural forces that occur between two phases, such as surface tension between air and water, interfacial tension between oil and water, and so on. Surfactants are amphiphilic molecules thus they can be absorbed at different interfaces (air/water or oil/water).[13-15]At the interface, the surfactant tries to align itself such that the *lyophobic* part remains in the air or oil phase, while the *lyophilic* part stays in the aqueous phase. When a surfactant moiety is dissolved in water, the polar head group interacts strongly with water molecules through dipole-dipole or ion-dipole interactions, assisting in solvation, while the hydrophobic group distorts water molecules' structure by breaking intermolecular hydrogen bonds. To minimize such distortion the surfactant moiety orients itself at the air-water interface in a manner such that the *hydrophilic* head group remains in contact with the aqueous medium and the *hydrophobic* part is oriented away from it. Thus the *amphipathic* structure of the surfactant allows it to concentrate at the surface of the aqueous medium thereby reducing the surface tension of water.

1.2.1. Classification of Surfactants

Depending upon the nature of solvents and physical parameters the chemical structure of the *lyophobic* and *lyophilic* parts of the surfactant varies.[14,16,17] For the case of highly polar solvents (such as water), the *hydrophobic* moiety can contain siloxane or hydrocarbon, or fluorocarbon chains, whereas in a less polar medium some of the above-mentioned moieties may not be suitable. Similarly, ionic or highly polar groups may act as *lyophilic* parts for more polar solvents (e.g. water), whereas they can behave as *lyophobic* moieties for the case of nonpolar solvents such as heptane.

The *hydrophobic* part of the surfactant contains often long-chain hydrocarbons, sometimes siloxanes or chemically modified hydrocarbon chains (halogenated or oxygenated). Depending on the choice of *hydrophilic* groups the surfactants can be classified as below; [18]

Table 1.1. Classification of surfactants.

CLASS	PROPERTIES	EXAMPLES
Anionic Surfactants	• The surface-active group bears a negative charge. • Relatively nontoxic. • Most widely used type of surfactants for shampoos, dishwashing liquids and laundering.	Most anionic surfactants are sulfates, sulfonates and soaps, such as sodium stearate ($CH_3(CH_2)_{16}COO^-Na^+$), sodium dodecyl benzene sulfonate ($CH_3(CH_2)_{11}C_6H_4SO_3^-Na^+$), sodium dodecyl sulfate ($CH_3(CH_2)_{11}SO_4^-Na^+$).
Cationic Surfactants	• The surface-active group bears a positive charge. • They serve as emulsifying agents. • They have germicidal properties thus are used in making of sanitizers.	Examples of cationic surfactants are; cetyl trimethylammonium bromide ($CH_3(CH_2)_{15}N^+CH_3)_3Br^-$), lauryl amine hydrochloride ($CH_3(CH_2)_{11}NH_3^+Cl^-$), trimethyl dodecyl ammonium chloride ($C_{12}H_{25}N^+(CH_3)_3Cl^-$) etc.
Zwitterionic Surfactants	• The surface-active group bears both positive and negative charges. • They are less common than other classes of surfactants. • Their mild nature makes them ideal for use in personal care or household cleaning products.	Examples of zwitterionic surfactants are; long-chain amino acids ($H_2NCHRCOOH$), sulfobetaine ($C_{13}H_{29}NO_3S$), dodecyl betaine ($C_{12}H_{25}N^+(CH_3)_2CH_2COO^-$).
Nonionic Surfactants	• The surface-active group bears no apparent charge. • They have extensive applications in the field of drug delivery. • They have excellent grease removal property, thus can be used in laundry and household cleaning products.	Most nonionic surfactants contain polyethylene glycol (PEG) chains. Examples include polyoxyethylene alcohols ($C_nH_{2n+1}(OCH_2CH_2)_mOH$), polyol esters, polyoxyethylene esters ($C_{17}H_{35}COO(CH_2CH_2)_nH$), etc.

1.2.2. Nonionic Surfactants

Nonionic surfactants are a fascinating class of surfactants, which has been under intense investigation by researchers in both the fields of chemical kinetics and biochemistry for the past few decades for their unusual polymeric structural properties.[19] They have vast applications in various fields like drug delivery, pharmaceuticals, industries such as food, paint, cosmetics and so on. There are two major categories of nonionic surfactants; polyoxyethylenes (general formula: $RO(CH_2CH_2O)_nH$) and polyhydric alcohols (general formula: $(CH_2CHOH)_n$).

Nonionic surfactants are usually highly stable and are not easily affected by the presence of acid, base or strong electrolytes. They do not dissociate in an aqueous medium and have a broad range of properties depending upon the *hydrophile-lipophile* balance (HLB). HLB describes the relationship between the water-soluble and oil-soluble parts of the nonionic surfactant moiety and has values in the range from 1 to 30 (or higher).

- For the case of $\mathrm{HLB} < 10$, the nonionic surfactant is oil soluble (*lipophilic*)
- For the case of $\mathrm{HLB} > 10$, the nonionic surfactant is water soluble (*hydrophilic*)

Surfactants with values in the range $8 < \mathrm{HLB} < 18$ are most commonly used in oil/water emulsions.

Another fundamental property of the surfactants is the formation of micelles in aqueous medium. In an aqueous medium, the surfactant monomers tend to form aggregates by orienting themselves in such a manner that the polar head groups remain in contact with the aqueous medium while the hydrophobic tails remain inside a core structure to stabilize the structure. The concentration at which the micelles start to form is known as the critical micelle concentration (CMC) of that specific surfactant. As these micellar structures behave differently from their monomer analogues they influence both solubility and viscosity of organic hydrocarbons and oils in aqueous medium. Depending upon the shape of the monomeric structures and concentration the micelles can be of different shapes, such as – spherical, rod-like, hexagonal, cubic and lamellar.

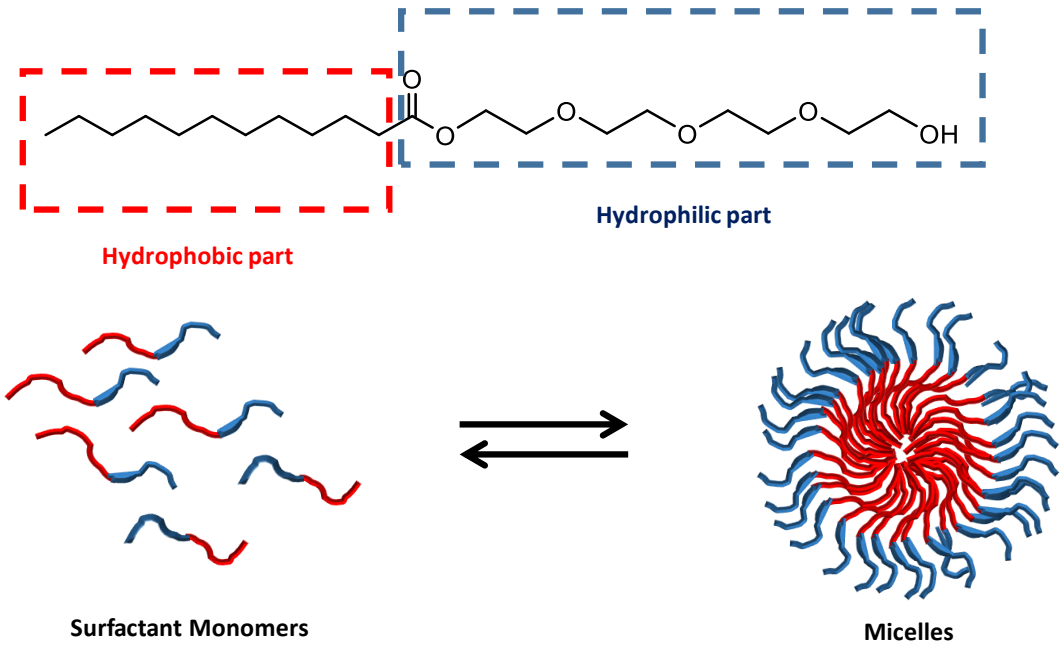

Figure 1.10. Cartoon illustration of micelle formation. Redrawn from reference [55].

For the case of ionic surfactants, the solubility increases with increasing temperature and is equal to the CMC value at a specific temperature known as kraft point (KP). The krafft point (KP) is an essential parameter as micelles only start forming at a temperature equal or above KP. Nonionic surfactants often do not exhibit KP their solubility decreases with increasing temperature. Nonionic surfactants may begin to lose their surface-active properties above a certain temperature known as cloud point.

1.3. Motivation behind the Project

Over the past decades, the self-assembly of surfactants, polymers and other amphiphilic molecules at the nematic LC-aqueous interface and the resulting optical and orientational changes of LC has been studied extensively.[20-31] While, ample literature is available on surface-driven anchoring transitions of LC mesogens at the aqueous-LC interface in presence of ionic surfactants, there are fewer reports on nonionic surfactants. Some of the key conclusions from the past studies on surfactants can be summarized as - i) Only amphiphiles with hydrophobic tails having more than 8 carbon atoms can induce an anchoring change; ii) Bolaform (adopts a looped configuration at the interface) or branched surfactants do not induce any anchoring transition due to poorer packing efficiency; iii) The anchoring transition is caused by hydrophobic interactions between the amphiphiles' hydrocarbon chains and is unaffected by the nature of the hydrophilic head group; lastly iv) To induce a planar to homeotropic transition, the surfactant concentration required is typically 5 to10 times lower than its CMC.[32-34] Recently, there have been several studies in synthetic amphiphiles and cleavable polymers that can report targeted events by triggering a transitional change in the LC ordering and the effect of external stimuli on such systems.[35,36] Motivated by this, in our work, we are trying to explore the self-assembly of a cleavable nonionic surfactant (Surf-LTE) that was synthesized in our lab and its cleaved fragments at the aqueous-LC interface.

Cleavable surfactants are currently of growing interest due to their eco-friendly biodegradable nature.[37,38] Ester-based surfactants often serve as natural choices for biodegradable surfactants in the laboratory due to some advantages, such as – they follow relatively simpler synthetic strategies, their chemical hydrolysis is often pH-dependent and hydrolysis of lipophilic esters can be easily catalyzed by lipase. In our lab, we have synthesized a nonionic surfactant tetra (ethylene glycol) mono-n-dodecanoate (MW: 376.53 g/mol) which is a biodegradable surfactant. The structure of the surfactant is given as following,

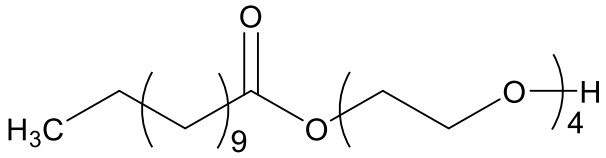

2-(2-(2-(2-hydroxyethoxy)ethoxy)ethoxy)ethyl dodecanoate

Figure 1.11. Chemical structure and IUPAC name of tetra (ethylene glycol) mono-n-dodecanoate (Surf-LTE).

Here, we have studied the changes in anchoring transitions triggered by the Surf-LTE monolayers adsorbed at the aqueous-LC interfaces on varying pH and salt concentrations. Further, we wanted to explore the change in its ordering transitions upon the presence of an external stimulus (chemical and enzymatic hydrolysis of the ester bond) and tried to compare it with the orientational transition induced by one of its synthetic components, lauric acid. polyethylene glycol (PEG) is widely utilized in nanoparticle-mediated drug delivery due to its immense biocompatibility and other properties.[39-42] In comparison to other charged or hydrophobic interfaces, polyethylene glycol (PEG) decorated interfaces have low levels of non-specific protein binding interactions, according to previous reports. PEGylation of the mesogens has been shown to reduce non-specific protein adsorption at the aqueous-LC interface (such as BSA).[43] We also observed a similar anchoring transition of the LC mesogens in presence of BSA at Surf-LTE (which is a PEG monoester) decorated monolayer adsorbed at the aqueous-LC interface.

Overall, the results of our study so far exhibit a straightforward and broad approach to the rational design of nonionic surfactant systems that can be used to program stimuli-responsiveness into nematic LC-aqueous interfaces. Also, this is a label-free method that can detect biomolecular events at the interface over time without the use of complex instruments. The results of this study can have applications in drug delivery thus enhancing its potential in the advancement of therapeutics.

Chapter 2

Experimental Section

2.1. Materials

The nonionic surfactant of interest, tetra (ethylene glycol) mono-n-dodecanoate (MW: 376.53 g/mol) was synthesized in our lab. Throughout the thesis, the surfactant is represented by the abbreviation Surf-LTE.

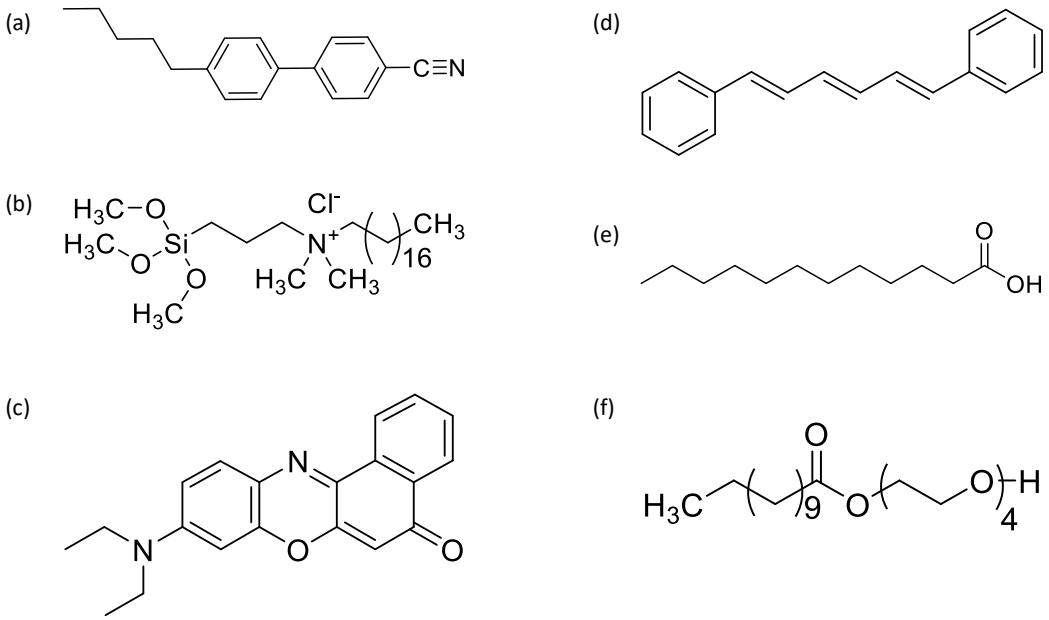

Figure 2.1. Chemical structures of commonly used reagents in the experiments (a) 5CB (4-Cyano-4'-pentylbiphenyl) (b) DMOAP (N,N-dimethyl-N-octadecyl-3-aminopropyltrimethoxysilyl chloride) (c) Nile Red (nile blue A oxazone) (d) DPH (1,6-diphenyl-1,3,5-hexatriene) (e) LA (lauric acid) (f) Surf-LTE (tetra (ethylene glycol) mono-n-dodecanoate).

Nematic liquid crystal 4-Cyano-4′-pentylbiphenyl (5CB), dimethyloctadecyl[3-(trimethoxysilyl)propyl]ammonium chloride (DMOAP), albumin from bovine serum (BSA), lipase from *Candida antarctica,* 1,6-diphenyl-1,3,5-hexatriene (DPH, 98%), nile blue A oxazone (nile red, 98%), sodium monohydrogen phosphate dihydrate ($Na_2HPO_4.2H_2O$), potassium phosphate dibasic (K_2HPO_4, >99%), citric acid (>99.5%) and sodium citrate dihydrate (>99%) were purchased from Sigma-Aldrich (St. louis, MO). Tetraethylene glycol (TEG, >95%, GC) and lauric acid (LA, >98%, GC) were purchased from Tokyo Chemical Industry Co., Ltd. Sulfuric acid (H_2SO_4, 95-98%), hydrogen peroxide (H_2O_2,30% w/v) and HPLC chloroform (>99.5%) were obtained from VETEC^{TM}, Sigma-Aldrich. HPLC acetone (>99.8%), hydrochloric acid (HCl, 37%), sodium hydroxide purified pellets (NaOH) and potassium chloride (KCl) were obtained from Merck (Mumbai, India). HPLC tetrahydrofuran (THF, >99.7%) was purchased from S D Fine Chemical Limited. Sodium chloride was obtained from HIMEDIA. Absolute ethanol (99.9%) was purchased from Changshu Hongsheng Fine Chemical Co., Ltd. Silicone isolators (12; 4.5 mm Diameter ×1.6 mm Depth ID, 25×54 mm OD, No PSA) were purchased from Grace Bio-Labs (Oregon, USA). Premium Microscope plain glass slides of finest grade were purchased from Fischer Scientific Company (Pittsburgh, PA, USA). Gold TEM grids (20 μm thickness, 50 μm wide bars, 283 μm grid spacing) were purchased from Electron Microscopy Sciences (Washington, PA, USA). Apart from the above-mentioned chemicals, eppendorf research plus micropipettes, micropipette tips from Tarsons, glass optical wells, coplin jars, kimwipes from Kimtech. Science brand, diamond tip glass cutter and BOROSIL glasswares were also purchased. A Milli-Q water purification system (Millipore, Bedford, MA) was used to deionize the water required for the preparation of all aqueous solutions.

2.2. Methods

2.2.1 Preparation of Buffers

a) 0.1 M Citrate Buffer (pH 2.7)

The reagents were weighed accordingly to prepare 200 mL of 0.1 M citrate buffer of approximately pH 3. 0.552 gm of sodium citrate dihydrate and 3.482 gm of citric acid were added to 200 mL of Milli-Q water. The pH was measured using a pH meter and was found to be 2.7.

i. 10 mM Citrate Buffer (pH 2.1)

20 mL of 0.1 M citrate buffer was taken in a suitable container. To this 180 mL of Milli-Q water was added to prepare 10 mM buffer solution. The final pH was adjusted to pH 2.1 by adding few drops of 5N HCl solution.

ii. 10 mM Citrate Buffer (pH 5.3)

20 mL of 0.1 M citrate buffer was taken in a suitable container. To this 180 mL of Milli-Q water was added to prepare 10 mM buffer solution. The final pH was adjusted to pH 5.3 by adding few drops of 5 M NaOH solution.

b) 0.1 M Phosphate Buffered Saline (PBS) Buffer (pH 7.1)

The reagents were weighed accordingly to prepare 200 mL of 0.1 M PBS buffer of approximately pH 6.8. 3.56 gm of sodium phosphate dibasic dihydrate, 0.48 gm of potassium dihydrogen phosphate, 16 gm of sodium chloride and 0.4 gm of potassium chloride were added to 200 mL of Milli-Q water. The pH was measured using a pH meter and was found to be 7.1.

i. 10 mM PBS Buffer (pH 7.6)

50 mL of 0.1 M PBS buffer was taken in a suitable container. To this 450 mL of Milli-Q water was added to prepare 10 mM buffer solution. The final pH was adjusted to pH 7.6 by adding few drops of 1 M NaOH solution.

ii. 10 mM PBS Buffer (pH 8.6)

20 mL of 0.1 M citrate buffer was taken in a suitable container. To this 180 mL of Milli-Q water was added to prepare 10 mM buffer solution. The final pH was adjusted to pH 8.6 by adding few drops of 1 M NaOH solution.

2.2.2. Preparation of aqueous solutions of Surf-LTE

A stock solution of the surfactant was prepared for performing the Polarised Optical Microscopy (POM) experiments. In a 25 mL round-bottomed flask calculated amount of surfactant was added; to this about 200 μL of acetone (HPLC grade) and required volume of PBS buffer (10 mM, pH 7.6) was added to make 10 mM Surf-LTE solution. The solution was kept on overnight (~12 hours) stirring at room temperature. The final volume was adjusted using the PBS buffer (10 mM, pH 7.6) to reach the final concentration of 10 mM.

All the surfactant solutions were prepared from this stock solution via further dilution using PBS buffer (10 mM, pH 7.6).

2.2.3. Preparation of Dye-Surfactant Solutions

a) DPH-Surf-LTE Solution

In a 25 mL round-bottomed flask calculated amount of surfactant was added; to this about 200 µL of acetone (HPLC grade) and required volume of PBS buffer (10 mM, pH 7.6) was added to make 50 mM stock solution. The solution was kept on overnight (~12 hours) stirring at room temperature. The final volume was adjusted using the PBS buffer (10 mM, pH 7.6) to reach the final concentration of 50 mM. All the surfactant solutions were prepared from this stock solution via further dilution using PBS buffer (10 mM, pH 7.6) as can be found in the following table (2.1).

Table 2.1. Preparation of aqueous Surf-LTE solutions.

Concentration (mM)	Volume of stock Surf-LTE solution added (µL)	Volume of PBS buffer (pH 7.6) added (µL)
0.1	1.0	499
0.25	2.5	497.5
0.4	4.0	496
0.55	5.5	494.5
0.7	7.0	493
0.85	8.5	491.5
1	10	490
3	30	470
5	50	450
7	70	430
9	90	410
11	110	390
13	130	370
15	150	350
17	170	330
19	190	310
21	210	290
23	230	270
25	250	250
27	270	230
30	300	200

10 mM DPH solution was prepared using THF as the solvent. 1 µL of the DPH solution was added to all the diluted surfactant solutions and the solutions were kept in dark for 3 hours before performing the fluorescence measurements.

b) NR-Surf-LTE Solution

In a 25 mL round-bottomed flask calculated amount of Surf-LTE was added; to this about 200 μL of acetone (HPLC grade) and required volume of PBS buffer (10 mM, pH 7.6) was added to make 10 mM stock solution. The solution was kept on overnight (~12 hours) stirring at room temperature. The final volume was adjusted using the PBS buffer (10 mM, pH 7.6) to reach the final concentration of 10 mM.

1 mg/mL nile red (NR) dye solution was prepared using acetone (HPLC grade). The solution was found to be violet in colour. Adequate volume of the NR solution was added to the freshly prepared Surf-LTE solution to reach the final concentration of 100 μM with respect to NR. The colour of the solution turned pink. The solution was kept on continuous stirring for 24 hours. Finally, the solution was centrifuged at 10,000 rpm for 15 mins before performing the fluorescence measurements.

2.2.4. Preparation of Glass Microscope Slides

a) Cleaning of glass slides

'Piranha' solution (70% H_2SO_4, 30% H_2O_2) was used to clean the microscope glass slides.[44] In short, the glass slides are carefully immersed in piranha solution inside a glass container. The container is then placed inside a water bath and is heated at 80ºC for 1 hour. The glass slides are then sequentially washed with Milli-Q water, ethanol and dried using N_2 gas. The cleaned slides are then placed inside the oven and dried for 3 to 4 hours maintaining the temperature at 100ºC.

b) Treatment with DMOAP

The cleaned slides were immersed in a 0.1% (v/v) dimethyloctadecyl[3-(trimethoxysilyl)propyl]ammonium chloride (DMOAP) solution for 30 minutes. Excess DMOAP was removed by rinsing the glass slides with Milli-Q water. The slides are immediately dried using N_2 gas and kept in the oven for 4 hours at 100ºC, allowing the crosslinking of DMOAP.[45]

2.2.5. Preparation of Doped LC Mixtures

a) Surf-LTE doped LC

A measured amount of Surf-LTE was dissolved in chloroform (HPLC grade) to prepare a 1mg/mL stock solution. To make the doped solutions required amount of the stock solution was added to 10 μL 5CB. The solutions were kept under high vacuum for 5 to 6 hours such that all the chloroform present inside the mixtures evaporate. The following table (2.2) describes the compositions of the doped mixtures (For details see Appendix):

Table 2.2. Preparation of Surf-LTE doped LC mixtures.

Weight Percentage (wt%)	Volume of LC (μL)	Volume of Surf-LTE(μL)
0.01	10	1.01
0.05	10	5.05
0.1	10	10.1
0.5	10	50.5
1	10	101
3	10	303

b) Lauric Acid doped LC

Measured amount of lauric acid (LA) was dissolved in chloroform (HPLC grade) to prepare a 1mg/mL stock solution. To make the doped solutions required amount of the stock solution was added to 10 μL 5CB. The solutions were kept under high vacuum for 5 to 6 hours such that all the chloroform present inside the mixtures evaporate. The following table describes the compositions of the mixtures (For details see Appendix):

Table 2.3. Preparation of LA doped LC mixtures.

Weight Percentage (wt%)	Volume of LC (μL)	Volume of LA (μL)
0.01	10	1.01
0.05	10	5.05
0.1	10	10.1
0.5	10	50.5
1	10	101
3	10	303

2.2.6. Preparation of LC thin films and optical cells

DMOAP coated glass slides were cut into small rectangular slides using a diamond glass cutter. These small pieces are then purged using N_2 gas to remove all the small glass particles and dust from the surface. Gold TEM grids are then placed on top of the glass slide pieces. For the POM experiments using an aqueous solution of Surf-LTE, the grids are then filled with approximately 0.2 to 0.3 μL 5CB using a hamiltonian syringe. Excess 5CB was removed to obtain a uniform interface. For the case of doping experiments, the grids are filled with exactly 0.2 μL of the respective doped 5CB solution using a micropipette. After use, the grids are rinsed with ethanol solution until fully cleaned and then dried in the oven overnight at 100ºC.

2.3. Instrumentation

2.3.1. Spectroscopic Measurements

a) UV-VIS spectrophotometer

All absorption measurements were performed using the spectrophotometer UV 3000^+ (Lab India, Analytical, Double beam, Version 3.5) with quartz cuvettes (1 cm path length). For DPH, the maximum absorption was observed at 356 nm (λ_{max}) and for nile red, the peak came at 536 (λ_{max}) nm (For details see Appendix).

b) Spectrofluorometer

All fluorescence measurements were performed using the spectrofluorometer RF-6000 (Shimadzu Corporation) with quartz cuvettes (1 cm path length). For experiments with DPH, the excitation wavelength was set at 356 nm and the emission was recorded at 430 nm (excitation and emission slit bandwidths were 1.5 and 1 nm, respectively). For measurements with nile red, the excitation wavelength was set at 536 nm and the spectra were recorded from 550 to 700 nm (excitation and emission slit bandwidths were 3 and 5 nm, respectively).

2.3.2. Optical Characterization of LC films

The optical characterization of LC films was done using a Zeiss Polarizing Optical Microscope (Scope.A1) in transmission mode. The microscope is equipped with cross

polars using objectives of magnification 5X, 50X, 100X and 200X. Each image was captured using an AxioCam camera equipped with a 5X objective lens (exposure time was set at 80 ms).

2.3.3. Quantification of LC response

To measure the grayscale intensity of the POM images, ImageJ software was used. The average grayscale intensity and the corresponding error for each time point was determined by taking the average of the grayscale intensity of nine different TEM grid squares.

Chapter 3

Results & Discussions

3.1. CMC Determination

Critical micelle concentration (CMC) is an essential parameter of any surfactant or amphiphilic molecule. Near CMC, the properties of surfactant solutions change drastically, such as there is a drop in electrical conductivity upon the formation of self-assembled micelles; increase in turbidity and stability in surface tension value, etc. To determine the CMC of the synthesized surfactant Surf-LTE, we have proceeded with the fluorescent probe method (DPH assay). DPH assay is an example of fluorescent turn-off probe method, where there is negligible or almost no fluorescence emission observed in solution but strong emission is observed upon micelle formation. Previous reports have shown that CMC does not depend on the concentration of the DPH dye.[46-49]

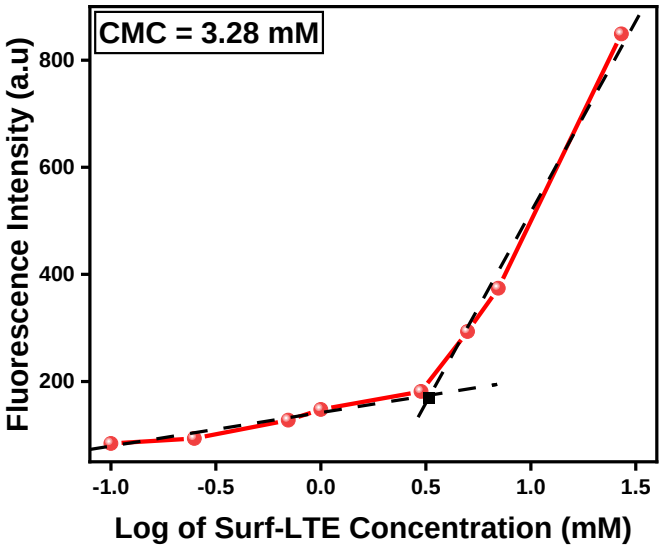

Figure 3.1. Fluorescence intensity vs. logarithm of Surf-LTE concentration (mM). The intersection of the two tangents drawn in the graph yielded the CMC.

The fluorescence intensity of DPH is highly enhanced upon incorporation into the hydrophobic core of the micelles. Thus with increasing concentration of Surf-LTE in solution, more micelles form and hence fluorescence intensity gradually increases. After a certain concertation, all the DPH molecules are bound and there is no further increase of fluorescence intensity. A plot of fluorescence intensity vs logarithm of surfactant concentration (mM) is drawn. The intersection of the two tangents drawn in the graph yielded the CMC. The CMC of Surf-LTE was found to be 3.28 mM at room temperature (25ºC) conditions.

3.2. Polarized Optical Microscopy (POM) experiments

All the POM experiments were carried out at room temperature (25ºC) conditions. Two major sets of experiments were performed - with doped LC systems and with aqueous solutions of surfactants. The experiments were performed in different buffer mediums (PBS and Citrate buffers of varied pH). 5CB was used in all of the polarized optical microscopy (POM) experiments in its nematic phase.

3.2.1. Experiments with Doped LC systems

The first set of experiments were carried out using doped 5CB mixtures with Surf-LTE and lauric acid. The weight percentages were chosen in a manner that the mixture retained the nematic phase behaviour of 5CB at room temperature (25ºC).

a) Optimization of doping concentrations of Surf-LTE and Lauric acid

1. Surf-LTE doped LC

At first, we studied the change in the optical response of LC in presence of different Surf-LTE doped LC mixtures (0.01, 0.05, 0.1, 0.5, 1 and 3 wt%) at the aqueous-LC interface. Towards this, we added different Surf-LTE doped 5CB mixtures to the gold TEM grids which are supported on DMOAP functionalized glass slides, this resulted in a dark optical appearance under the crossed polars. The dark appearance was due to the impartment of homeotropic alignment on the LC mesogens by the hydrophobic interactions of DMOAP present on the glass slides. Next, we submerged these systems in 2 mL of 10 mM PBS buffer (pH 7.6). For 0.01, 0.05 and 0.1 wt% doped systems we observed a bright optical appearance under the crossed polars, which was stable up to 2 hours. On the other hand, for 0.5, 1 and 3 wt% doped systems, we observed a dark optical signal which was stable for up

to 2 hours. At very high doping concentrations (such as 5 wt%) we observe textures similar to isotropic phase. (For details see Appendix).

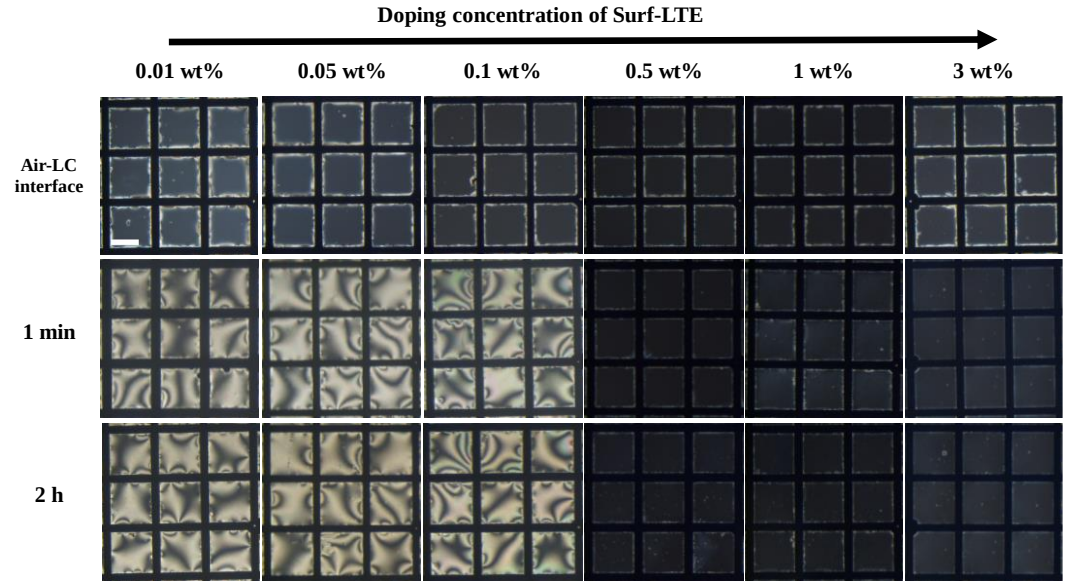

Figure 3.2. POM images of Surf-LTE doped 5CB film (0.01, 0.05, 0.1, 0.5, 1 and 3 wt%) at air-LC interface and aqueous-LC interface (10 mM PBS buffer medium at pH 7.6). Time indicates the instant at which images were captured after the introduction of PBS buffer on Surf-LTE doped LC film. Scale bar = 200 µm.

We may argue that with lower doped concentrations, the areal density of surfactant adsorbed at the interface was not enough to induce a transition from planar to homeotropic orientation of the LC mesogens, thus resulting in a bright optical response. Similarly, with increasing doping concentrations the amount of surfactant adsorbed at the interface may surpass the critical value where it can induce a homeotropic alignment on the LC mesogens resulting in a dark optical response. The homeotropic alignment is induced by the hydropic interactions between alkyl chains of surfactant and 5CB. In addition to the hydrophobic interactions, we predict that the presence of tetra ethylene glycol moiety assisted the homeotropic orientation by forming a stable monolayer with the help of intermolecular hydrogen bonding with water molecules.

2. Lauric acid doped LC

Next, we studied the change in the optical response of LC in presence of different lauric acid doped LC mixtures (0.01, 0.05, 0.1, 0.5, 1 and 3 wt%) at the aqueous-LC interface. We performed these experiments similarly as above. For 0.01, 0.05 and 0.1 wt% doped systems we observed a bright optical appearance under the crossed polars, that was stable

for up to 2 hours. 0.5 and 1 wt% doped systems initially gave a dark optical appearance which was not stable and turned into a bright optical signal within 2 hours. For 3 wt% we observed a dark optical signal which was stable for up to 2 hours.

Lauric acid has a pK_a of 5.3; i.e. it will partially dissociate into laurate ions at pH 7.6. Previous reports have explained the ordering transition induced by the long-chain fatty acids at the aqueous-LC interface.[51, 52] Lauric acid in its acidic form will try to stay dissolved inside the bulk LC medium, resulting in random alignment of the LC mesogens and thereby a bright optical signal. At higher pH (> 5.3) as it starts to dissociate, the laurate ions will move to the aqueous interface from bulk LC medium to avoid electrostatic repulsion. Thus a stable monolayer at the interface is formed (due to the attractive interaction between laurate ions and lauric acid molecules), which in turn will impart a homeotropic alignment on the LC mesogens resulting in a dark optical signal. With the increase of adsorbed molecules at the interface, the laurate ions start to repel each other because of the electrostatic interactions. This results in desorption of the laurate ions from the interface and to move to the bulk aqueous medium.

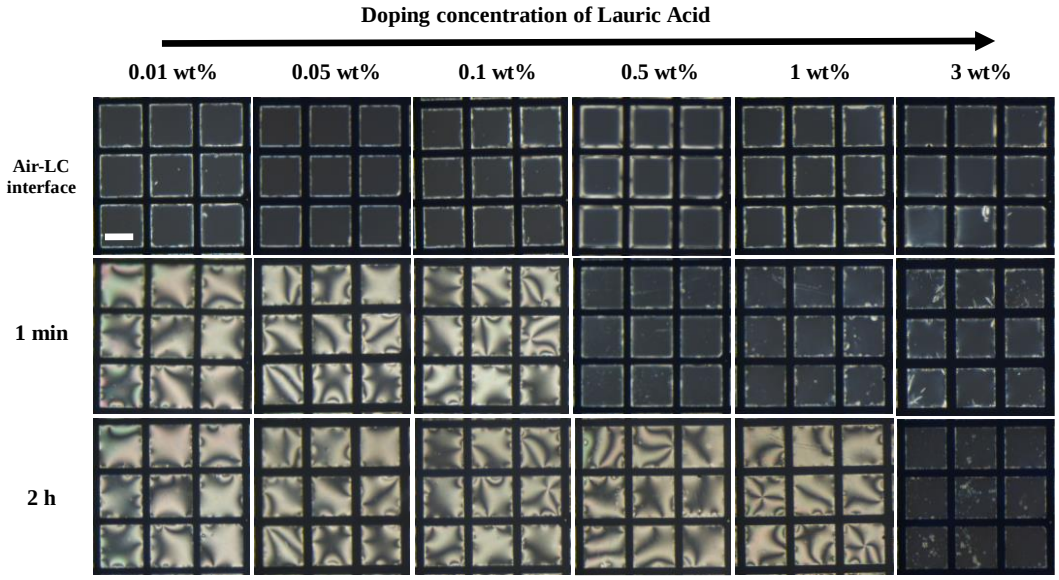

Figure 3.3. POM images of LA doped 5CB film (0.01, 0.05, 0.1, 0.5, 1 and 3 wt%) at air-LC interface and aqueous-LC interface (10 mM PBS buffer medium at pH 7.6). Time indicates the instant at which images were captured after the introduction of PBS buffer on LA doped LC film. Scale bar = 200 µm.

Now, at very low doping concentrations (0.01, 0.05 and 0.1 wt%), there are very few numbers of lauric acid molecules present inside the bulk LC medium. Thus even at pH 7.6,

where lauric acid dissociates into laurate ions; the ions remain very far apart to exhibit any electrostatic repulsion on each other. Thus we obtain a bright optical signal under the crossed polars as LC mesogens remain randomly oriented. But with increasing doping concentration (0.5 and 1 wt%) the laurate ions after forming a stable monolayer at the interface start to desrob and move to the bulk aqueous medium. Thus we observe a change from dark to bright optical signal due to the anchoring transition from homeotropic to planar of LC mesogens. Now, at a very high doping concentration (3 wt%) a large number of laurate ions and lauric acid molecules remain at the interface forming a stable monolayer inducing a homeotropic anchoring of the LC mesogens, resulting in a dark optical appearance under the crossed polars (for up to 2 hours).

b) Effect of pH on LC ordering of Surf-LTE and Lauric acid doped LC

We studied the effect of pH variation for both 0.5 wt% Surf-LTE and 0.5 wt% lauric acid doped LC systems, as we observed a change in the stability of homeotropic orientation of the LC mesogens at this doping concentration at pH 7.6.

1. Surf-LTE doped LC

We performed the experiments with 0.5 wt% Surf-LTE doped LC system in four different pH mediums (pH 2.1, 5.3, 7.6 and 8.6). No difference in the optical signal was observed. The LC gave dark optical response which was stable for up to 2 hours in all pH mediums. We can argue that the Surf-LTE structure is highly stable in the aqueous medium, thus protonation and deprotonation cannot occur under such mild conditions of pH variation. The presence of tetra ethylene glycol chains adds to the overall stability of the structure.

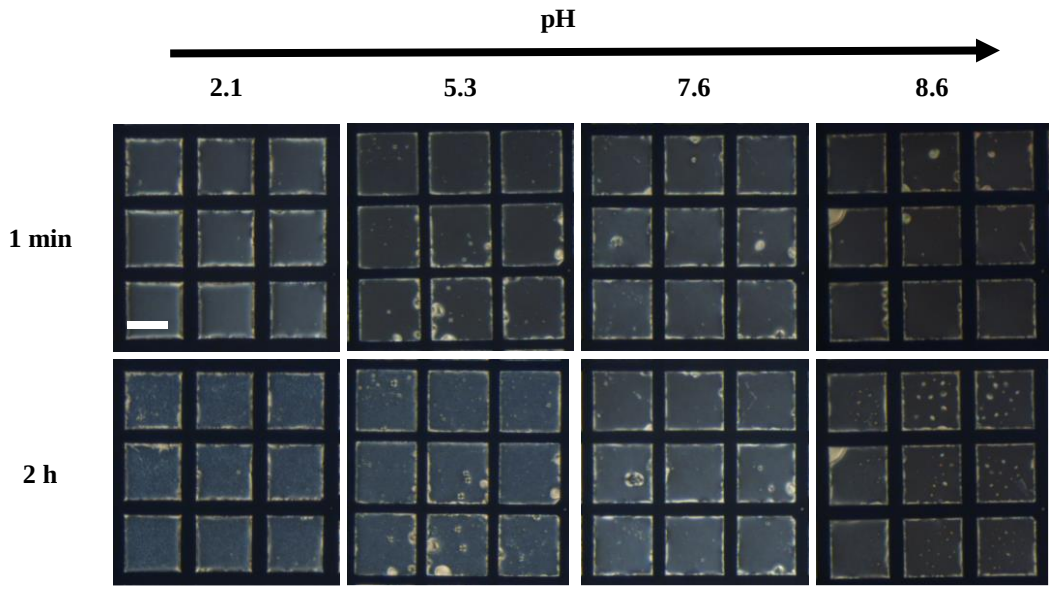

Figure 3.4. POM images of 0.5 wt% Surf-LTE doped 5CB film at aqueous-LC interface at different pH mediums (2.1, 5.3, 7.6 and 8.6). Time indicates the instant at which images were captured after the introduction of buffer on Surf-LTE doped LC film. Scale bar = 200 μm.

2. Lauric acid doped LC

We performed similar experiments with 0.5 wt% lauric acid doped LC system in four different pH mediums (pH 2.1, 5.3, 7.6 and 8.6). Here, we observed the systems at pH 2.1 and 5.3 gave a bright optical response which was stable for up to 2 hours. Whereas, the systems at pH 7.6 and 8.6 gave an initial dark optical response which became bright within 2 hours.

Lauric acid has a pK_a of 5.3; i.e. at pH < 5.3 lauric acid will remain protonated and at a pH > 5.3 it will be deprotonated. Now past reports have established the effect of pH variation on fatty acid systems.[50, 51] Our observations with 0.5 wt% doped lauric acid system gave similar optical responses at the aqueous-LC interface.

At acidic pH mediums (pH 2.1 and 5.3) lauric acid remains in its protonated form. Due to the presence of long hydrophobic tails (12 carbon aliphatic chain length) lauric acid molecules remain dissolved in the bulk LC medium, resulting in a random alignment of the LC mesogens at the aqueous-LC interface. Thus, we obtain a bright optical appearance under the crossed polars which is stable for up to 2 hours.

With increasing pH of the medium (i.e. at pH values > 5.3 such as 7.6 and 8.6) lauric acid molecules start dissociating into laurate ions. The integrated structures at the bulk LC

break due to electrostatic repulsion between anionic head groups, and molecules begin to move freely. Since carboxylate ions are more water-soluble than their acidic analogues, they have a higher tendency to move to the aqueous-LC interface from bulk LC medium. Presence of the attractive forces between the lauric acid molecules and laurate ions (electrostatic and intermolecular hydrogen bonding) a stable monolayer can be adsorbed at the interface which will, in turn, impart homeotropic anchoring on the LC mesogens at the interface, thus resulting in a dark optical signal. Now with an increasing number of adsorbed molecules at the interface, if the critical value is surpassed, molecules start desorbing from the aqueous interface to the bulk aqueous medium. Thus an anchoring transition from homeotropic to planar occurs, which results in a bright optical response. Thus we observed a transition in the optical signal from dark to bright at pH 7.6 and 8.6 (observed for up to 2 hours).

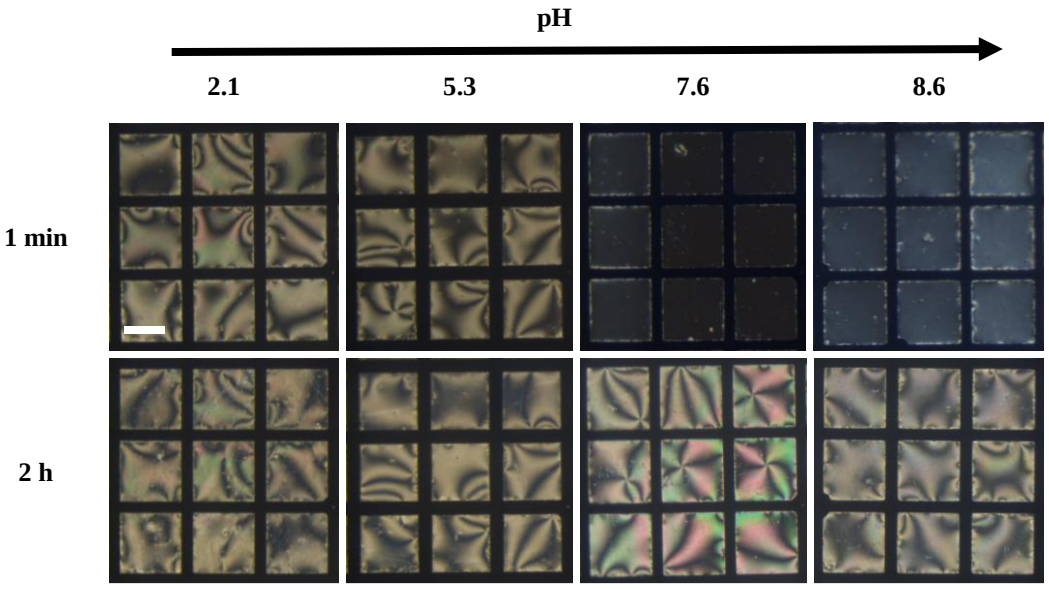

Figure 3.5. POM images of 0.5 wt% LA doped 5CB film at aqueous-LC interface at different pH mediums (2.1, 5.3, 7.6 and 8.6). Time indicates the instant at which images were captured after the introduction of buffer on LA doped LC film. Scale bar = 200 μm.

c) Chemical hydrolysis of Surf-LTE in presence of HCl and NaOH

After confirming the stability of the self-assembled Surf-LTE monolayer at the aqueous-LC interface, we wanted to study the chemical hydrolysis of the system using HCl and NaOH. We hypothesized that there should be some change in the optical appearance upon

hydrolysis as cleavage of the ester bond should impart a change in the structural orientation of the Surf-LTE at the interface. We first studied the fluorescence quenching of NR-Surf-LTE in presence of HCl and NaOH and obtained the minimum concentration of HCl and NaOH required to hydrolyze the system. We observed, 0.231 N HCl and 0.5 M NaOH quenched the fluorescence emission of 3mM NR-Surf-LTE solution and for the case of 0.5 mM NR-Surf-LTE solution 0.091 N HCl and 0.375 M NaOH were required. We tried to imitate the same conditions in our polarized optical microscopy (POM) experiments.

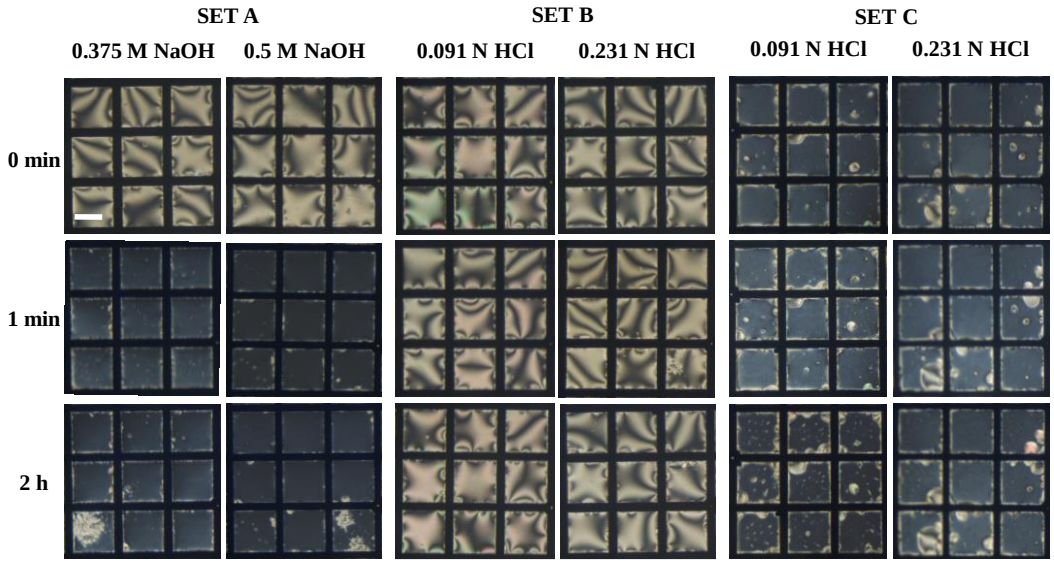

Figure 3.6. SET (A) POM images of 5CB film in presence of NaOH (0.375 M and 0.5 M). SET (B) POM images of 5CB film in presence of HCl (0.091 N and 0.231 N). SET (C) POM images of 0.5 wt% Surf-LTE doped 5CB film in presence of HCl (0.091 N and 0.231 N). All systems are in a 10 mM PBS buffer medium of pH 7.6. Time indicates the instant at which images were captured after the introduction of aqueous solutions on LC film. Scale bar = 200 μm.

First, we checked the stability of planar orientation of 5CB mesogens in PBS buffer medium (pH 7.6) in presence of HCl and NaOH. For both concentrations of HCl (0.231 N and 0.091 N) no change in the optical signal was observed. The bright optical appearance was stable for up to 2 hours. Whereas for the case of NaOH, we observed a change in the optical signal from bright to dark for both concentrations (0.5 M and 0.375 M) in PBS buffer medium (pH 7.6). The dark optical signal was stable for up to 2 hours. Thus we proceeded with HCl for the next set of experiments.

We added 0.5 wt% Surf-LTE doped LC in gold TEM grids supported on DMOAP coated

glass slides and submerged the system in 10 mM PBS buffer medium at pH 7.6. This gave a dark optical signal as was observed previously. Next, we added HCl and observed no change in the optical signal for both 0.231 N and 0.091 N concentrations of HCl. Thus, we could not observe the chemical hydrolysis using POM experiments and decided to proceed with the enzyme Lipase, to check the biochemical hydrolysis of Surf-LTE.

d) Determination of Lipase Activity on Surf-LTE

We studied the enzymatic activity of lipase on 0.5 wt% Surf-LTE doped LC system. The enzyme unit of lipase is 0.3 U/mg (for the particular sample we purchased). Thus we calculated 0.135 μM to be the least concentration of lipase to observe biochemical hydrolysis in 0.5 wt% Surf-LTE doped LC system (see Appendix for details). We observed a slow but gradual change in the optical signal of LC from dark to bright at the aqueous-LC interface under the crossed polars for up to 1 hour. Previous reports have shown that lipase does not induce any orientational transition of the LC mesogens.[52] Thus it can be confirmed that the bright optical signal was observed due to the orientational transition of LC mesogens from homeotropic to planar alignment. As lipase can hydrolyze Surf-LTE into lauric acid and tetra ethylene glycol, we expect at a neutral pH medium (pH 7.6) lauric acid molecules will dissociate into laurate ions which will, in turn, desorb from the interface to the bulk aqueous medium, as was explained earlier in details. Thus with a less areal density of amphiphilic molecules at the interface may change the orientational transition of the LC mesogens from homeotropic to planar, thereby resulting in a bright optical appearance under the crossed polars.

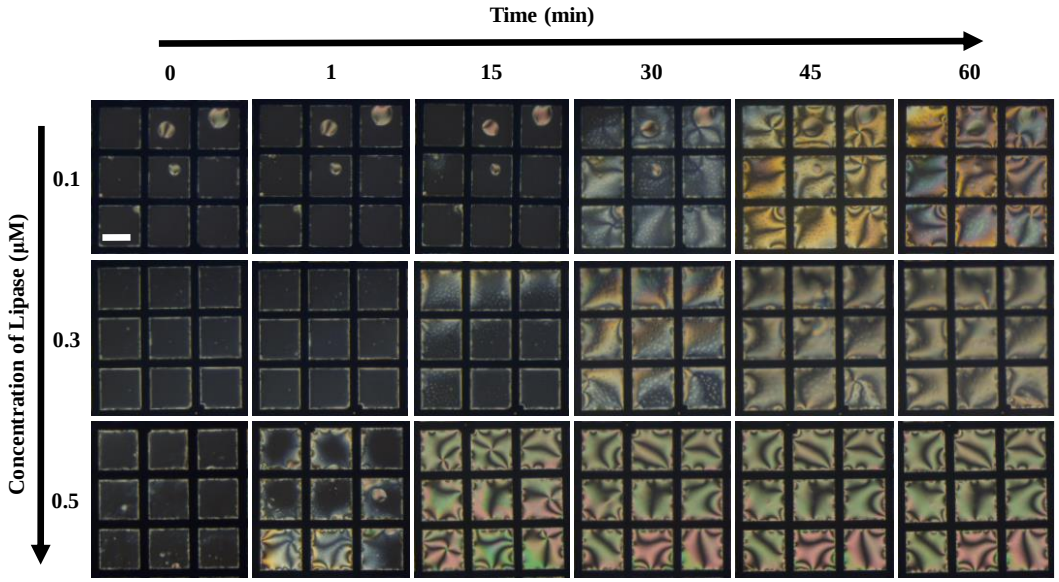

Figure 3.7. POM images of 0.5 wt% Surf-LTE doped 5CB at aqueous-LC interface in 10 mM PBS buffer medium (pH 7.6) showing dynamic response of LC due to the presence of different concentrations of lipase (0.1, 0.3 and 0.5 μM) at different time

Next, we wanted to check the sensitivity of lipase action. We performed the same set of experiments with 0.1, 0.3 and 0.5 μM lipase solutions. We observed that all solutions when added to 0.5 wt% Surf-LTE doped 5CB filled TEM grids changed the optical signal from dark to bright gradually (observed up to 1 hour); fastest conversion being with 0.5 μM lipase. This was also evident from the grayscale intensity vs time plot of the optical micrographs. The plot shows that as the lipase concentration increases, the transition in the optical signal from dark to bright becomes faster. Thus plotting the average grayscale intensity of all the optical micrographs help in quantifying the rate of biochemical hydrolysis due to lipase activity at the interface. Thus we can also detect the enzymatic activity of lipase using Surf-LTE at the aqueous-LC interface platform.

Table 3.1. Comparative analysis of initiation of hydrolysis of Surf-LTE for different concentrations of lipase.

Concentration of Lipase (μM)	Initiation time (min)
0.1	25
0.3	15
0.5	1

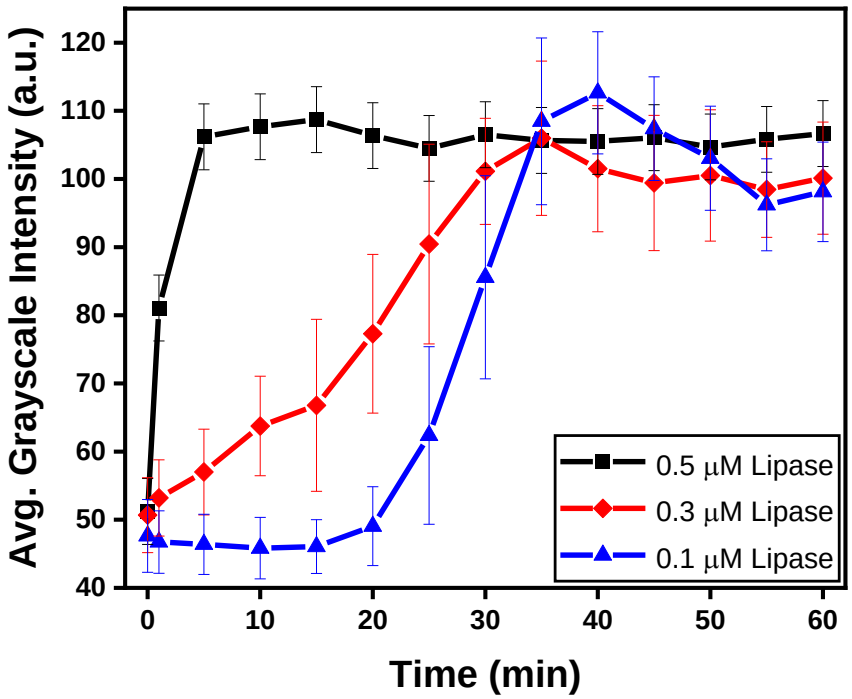

Figure 3.8. Quantification of lipase activity; Graph represents the average grayscale intensity of the POM images as a function of time at different concentrations of lipase by taking 9 squares in the TEM grid. The initial time point indicates 0 min, with no addition of lipase, in 10 mM PBS buffer medium (at pH 7.6).

e) Adsorption of BSA on Surf-LTE and Lauric acid laden aqueous-LC interfaces

Lastly, we studied the interaction of bovine serum albumin protein (BSA) with both 3 wt% Surf-LTE doped and 3 wt% lauric acid doped LC systems. We chose 3 wt% doping concentration since for both the systems, at 3 wt% doping concentration we have observed stable homeotropic anchoring of LC mesogens at the interface, resulting in a dark optical appearance under the crossed polars.

1. Surf-LTE doped LC

On addition of 0.5 μM BSA solution to the 3 wt% Surf-LTE doped LC system in 10 mM PBS buffer medium (7.6), we observed no change in the optical signal. The dark optical appearance under the crossed polars was stable (observed for up to 30 mins). We may assume that the tetra ethylene glycol chains of Surf-LTE molecules may saturate the

aqueous interface due to the formation of strong intermolecular hydrogen bonding and mask any effect of BSA present in bulk. Thus we observe no change in the optical response.

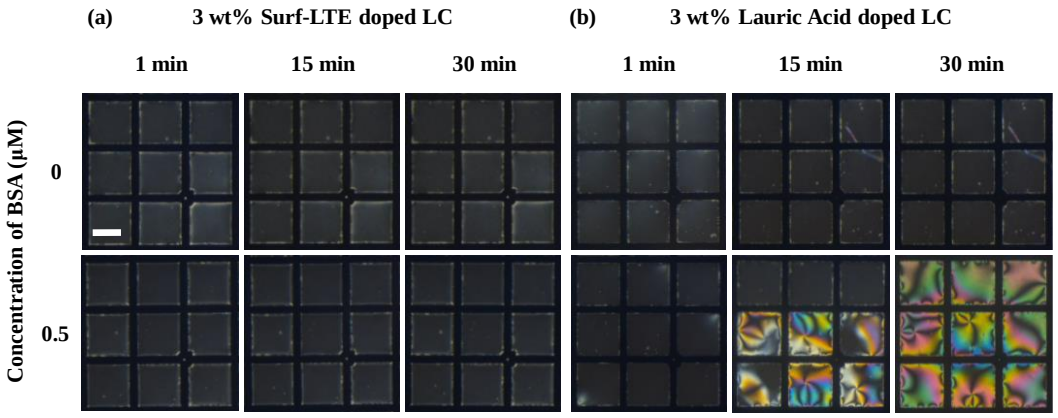

Figure 3.9. (a) POM images of 3 wt% Surf-LTE doped 5CB film in presence of 10 mM PBS buffer medium at pH 7.6 (top row) and in presence of an aqueous solution of 0.5 µM BSA (bottom row). (b) POM images of 3 wt% LA doped 5CB in presence of 10 mM PBS buffer medium at pH 7.6 (top row) and in presence of an aqueous solution of 0.5 µM BSA (bottom row). Time indicates the instant at which images were captured after the introduction of aqueous solutions on LC film. Scale bar = 200 µm.

2. Lauric acid doped LC

Now, we similarly added 0.5 µM BSA solution to the 3 wt% lauric acid doped LC system in 10 mM PBS buffer medium (7.6). Here, we observed a gradual transition in the optical signal from dark to bright. The optical signal turned completely bright after 30 mins and was stable afterwards. Previous studies have shown BSA has alkane binding sites consisting of nonpolar amino acids. We may assume that these alkane binding sites can have hydrophobic interactions with the alkyl chains of lauric acid molecules. Thus lauric acid molecules may desorb from the aqueous-LC interface, resulting in the bright optical appearance under the crossed polars.

3.2.2. Experiments with aqueous solutions of Surfactants

All the experiments were carried out at concentrations that are below CMC (3.28 mM) of Surf-LTE. High concentrations that are close to CMC or above caused turbidity and desorption of the LC mesogens from the interface to the bulk.

a) Optimization of Surf-LTE concentration

At first, we studied the change in the optical signal of the LC in presence of different concentrations of Surf-LTE solutions. Firstly, we added 5CB to the gold TEM grids which are supported on DMOAP coated glass slides, this generated a dark optical appearance under the crossed polars. The dark appearance was due to the impartment of homeotropic alignment on the LC mesogens at the air-LC interface by the hydrophobic interactions of DMOAP present on the glass slides. As a control, we next submerged the system in 10 mM PBS buffer (pH 7.6) and there was a change from dark to bright optical appearance which is because of the planar alignment caused by the interaction of water molecules with the LC mesogens.

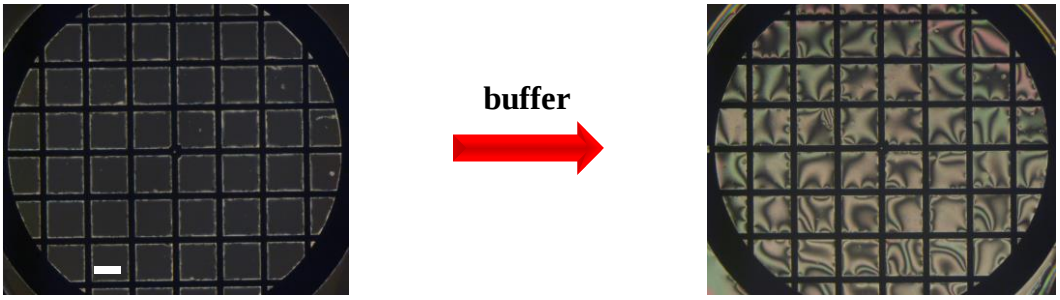

Figure 3.10. POM images of 5CB film before and after introduction of 10 mM PBS buffer medium at pH 7.6. Scale bar = 200 µm.

Next, we added a sufficiently high concentration of Surf-LTE and there was a change in the optical appearance from bright to dark due to the orientational transition of the LC mesogens from planar to homeotropic alignment. The hydrophobic interactions between the alkyl chains of the surfactant and 5CB imparted the perpendicular orientation of the LC mesogens at the aqueous-LC interface. In addition to the hydrophobic interactions, we predict that the presence of tetra ethylene glycol moiety assisted the homeotropic orientation by forming a stable monolayer with the help of intermolecular hydrogen bonding with water molecules.

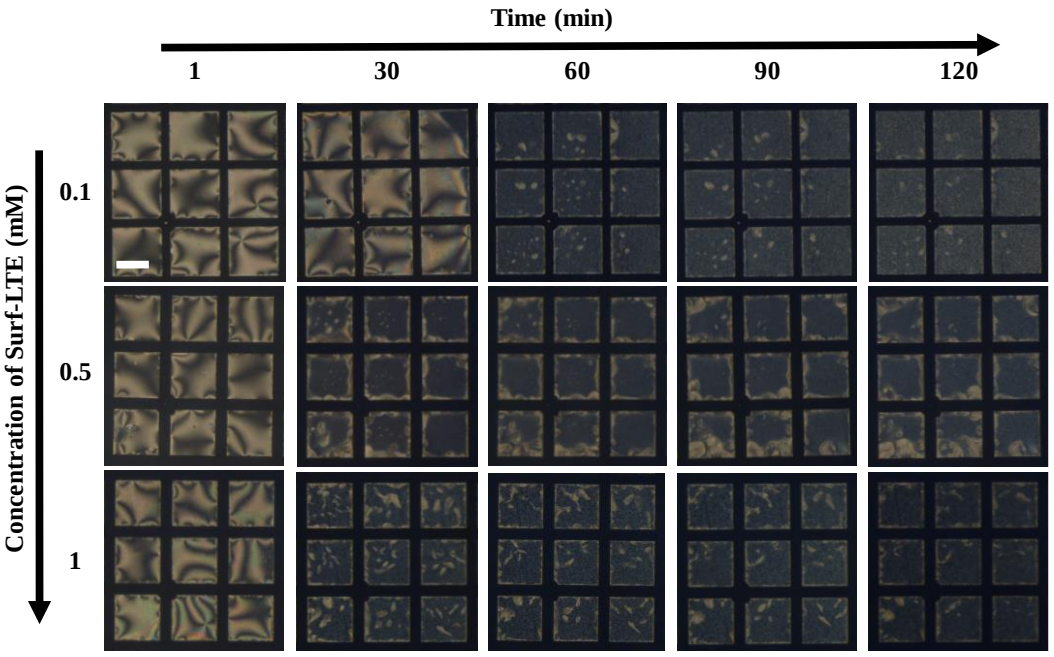

Figure 3.11. POM images of 5CB film after the introduction of aqueous solutions of Surf-LTE (0.1, 0.5 and 1 mM) at pH 7.6. Scale bar = 200 µm.

Next, we performed a series of experiments with Surf-LTE solutions of varying concentrations (0.1, 0.5, 1 and 2 mM). With the addition of Surf-LTE in the bulk, the bright appearance of the LC changed into a dark optical appearance. It is due to the stable self-assembled Surf-LTE monolayer at the aqueous-LC interface, as the hydrophobic interactions between the Surf-LTE and 5CB alkyl chains impart a homeotropic orientation on the LC mesogens. We observed that with 0.1mM Surf-LTE, LC gave a dark appearance at 60 mins; with 0.5 mM dark signal appeared within 30 mins; with 1 mM the optical signal became dark in 15 mins and with 2mM the solution became turbid and desorption of LC mesogens from the interface started right away (For details see Appendix). Thus, we proceeded with 0.5 mM Surf-LTE for the next set of experiments.

b) Effect of pH on LC ordering in presence of Surf-LTE

Next, we wanted to study the effect of changing the pH in the system. We performed the experiments with 0.5 mM Surf-LTE in four different pH mediums (pH 2.1, 5.3, 7.6 and 8.6). No difference in the optical signal was observed. It could be due to the fact that, the Surf-LTE structure is highly stable in the aqueous medium, thus protonation and deprotonation cannot occur under mild conditions.

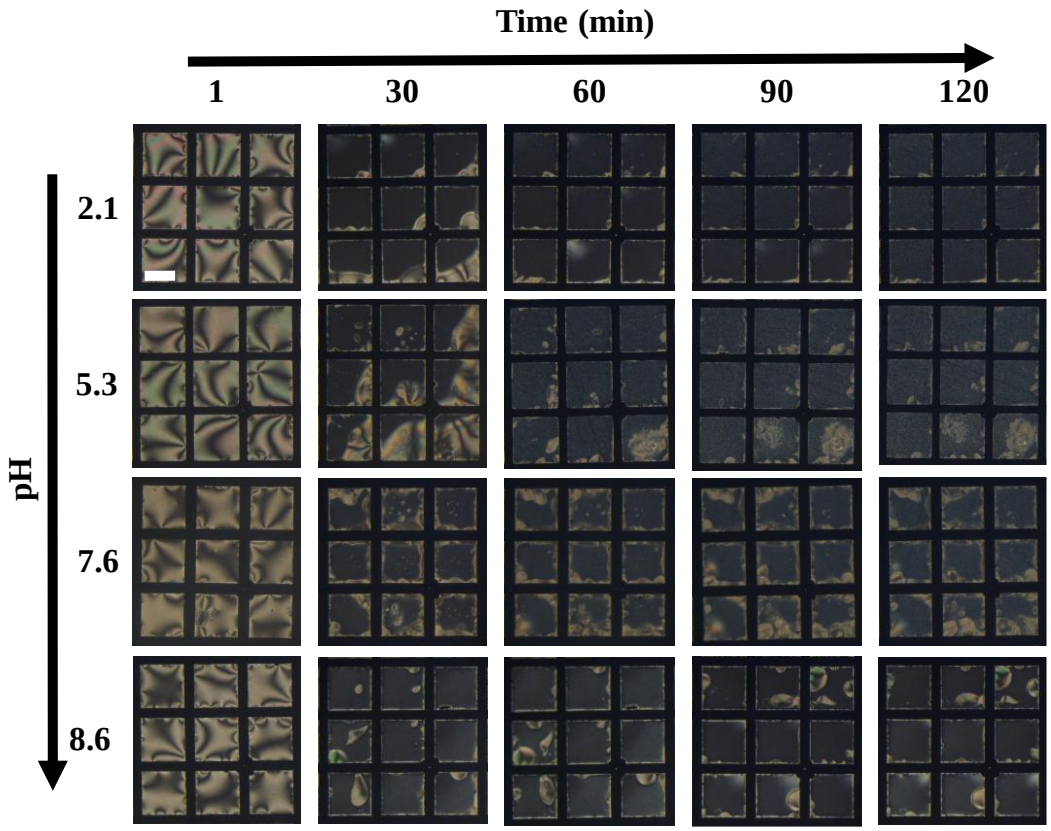

Figure 3.12. POM images of 5CB film after the introduction of aqueous solutions of Surf-LTE (0.5 mM) at different pH mediums (pH 2.1, 5.3, 7.6 and 8.6). Scale bar = 200

c) Effect of Ionic Strength on LC ordering in presence of Surf-LTE

Previous reports have shown that the addition of electrolytes can facilitate adsorption of ionic surfactants at the hydrophobic interfaces. Electrolytes screen the electrostatic repulsion among the ionic head groups of the surfactant systems, thereby stabilizing the system. Electrolytes have been reported to affect the LC ordering at aqueous-LC interfaces in case of ionic surfactants but have displayed no effect for the case of nonionic surfactants. Here, we have also observed no effect on the addition of 100 mM NaCl to a solution of 1mM Surf-LTE in PBS buffer medium at pH 7.6 on the LC ordering. We have performed control experiments, i.e. without the presence of NaCl salt and observed that there was no change in the homeotropic alignment of LC at the aqueous-LC interface.

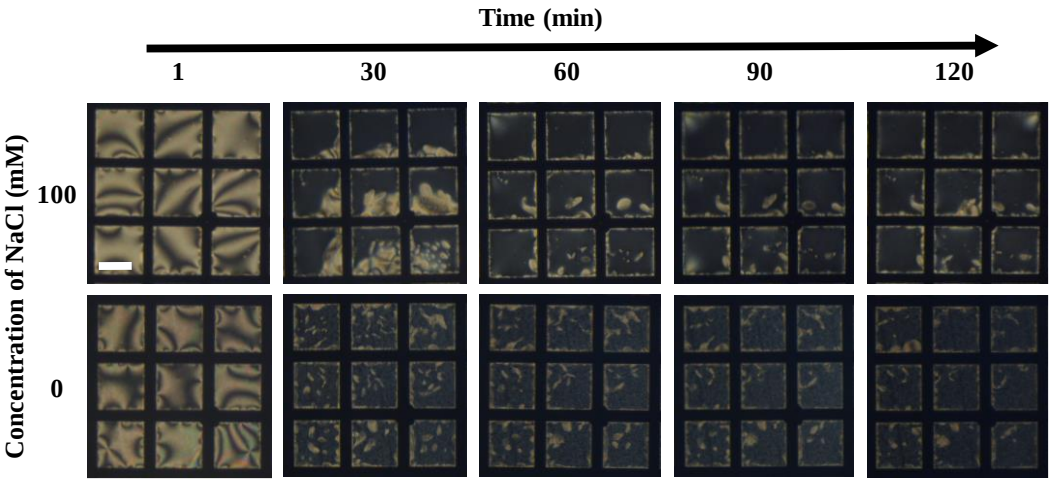

Figure 3.13. POM images of 5CB film in presence of an aqueous solution of Surf-LTE (1 mM) at pH 7.6 without (bottom row) and with (top row) the introduction of 100 mM NaCl. Scale bar = 200 µm.

d) Determination of Lipase Activity on Surf-LTE

We wanted to study the enzymatic activity of lipase on Surf-LTE. We incubated 0.5 mM aqueous solution of Surf-LTE with sufficient high concentration (0.5 mg/mL) of lipase for 90 mins. This mixture was then added to LC filled TEM grids, supported on DMOAP coated glass slides and confined in a silicone isolator (12; 4.5 mm Diameter ×1.6 mm Depth ID, 25×54 mm OD, No PSA). We observed a bright optical appearance of LC at the aqueous-LC interface under the crossed polars. As a control, we added 0.5 mM Surf-LTE solution onto the grid, which gave a dark optical appearance as was expected. Thus it can be confirmed that the bright optical signal was observed due to the orientational transition of LC mesogens from homeotropic to planar alignment, as previous reports have shown that lipase does not induce any orientational transition of the LC mesogens.[52] As lipase can hydrolyze Surf-LTE into lauric acid and tetra ethylene glycol, we expect at a neutral pH medium (pH 7.6) lauric acid molecules will dissociate into laurate ions which will, in turn, desorb from the interface to the bulk aqueous medium, as was explained earlier in details. Thus with a less areal density of amphiphilic molecules at the interface may change the orientational transition of the LC mesogens from homeotropic to planar, thereby resulting in a bright optical appearance under the crossed polars.

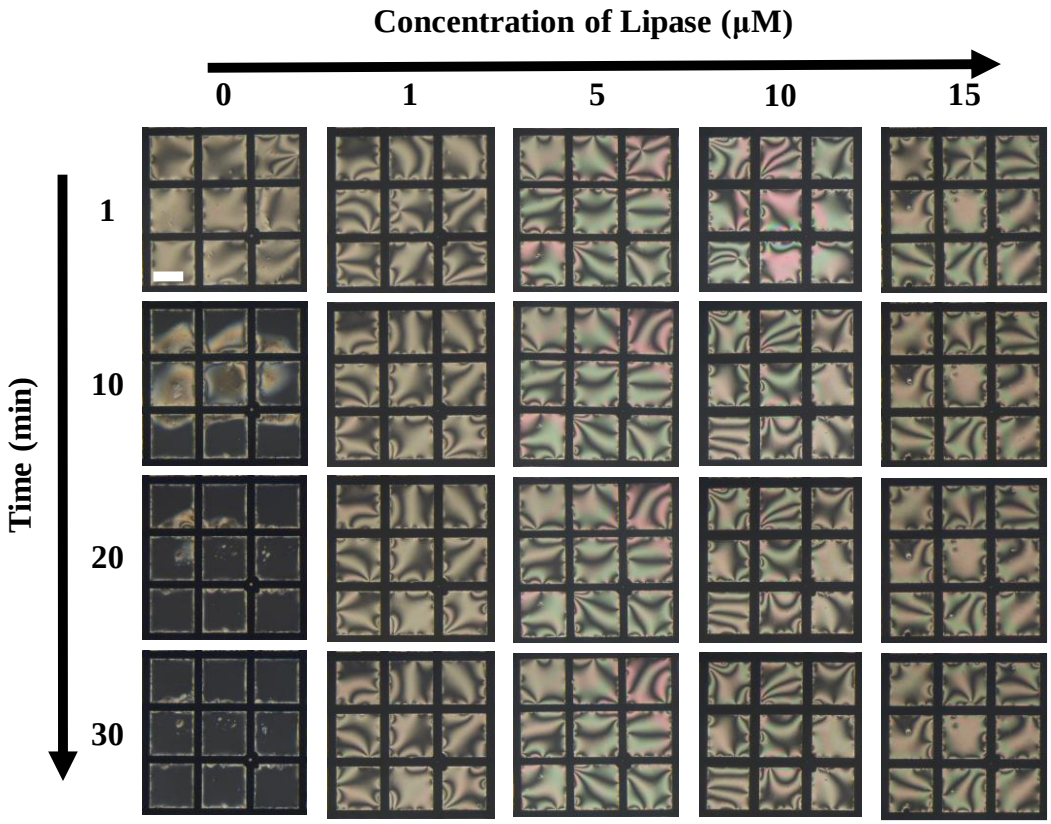

Figure 3.14. POM images of 5CB in presence of preincubated mixtures of 0.5 mM Surf-LTE and different concentrations of lipase solution (0,1,5,10 and 15 µM) at pH 7.6. Scale bar = 200 µm.

Next, we wanted to optimize the minimum concentration of lipase required to induce a planar orientation. We incubated 0.5 mM Surf-LTE with different concentrations of lipase (1, 5, 10 and 15 µM) for 90 mins and performed the same set of experiments. We observed that all solutions when added to 5CB filled TEM grids gave a bright optical signal (observed up to 30 mins). Thus we can detect the enzymatic activity of lipase using Surf-LTE at the aqueous-LC interface platform up to a concentration of 1µM.

3.3. Fluorescence quenching experiments

We conducted fluorescence quenching experiments that are in parallel with the polarized microscopy experiments to observe ester hydrolysis of Surf-LTE. We have proceeded in two pathways, the first being the chemical hydrolysis using NaOH and HCl; the second is the biochemical hydrolysis using lipase. We had prepared a 10 mM aqueous Surf-LTE stock solution containing 100 µM nile red dye, from which we made 3mM and 0.5 mM

diluted solutions for conducting the fluorescence experiments. In the case of nile red assay, there is almost no fluorescence emission observed in an aqueous medium, but a strong fluorescence emission is observed upon the formation of stable Surf-LTE micelles (fluorescence intensity of NR is highly enhanced upon incorporation into the hydrophobic core of the micelles).

a) Chemical hydrolysis of Surf-LTE

We expect that in presence of any strong base (NaOH) or acid (HCl) the ester bond present in Surf-LTE will undergo chemical hydrolysis, resulting in the breakdown of the micellar structure. Thus the intensity of fluorescence emission will decrease. We observed such fluorescence quenching for both 0.5 mM and 3 mM aqueous solutions of Surf-LTE. For 3 mM Surf-LTE system, 0.231 N HCl and 0.5 M NaOH caused complete fluorescence quenching. For the case of 0.5 mM Surf-LTE system, it took 0.091 N HCl and 0.375 M NaOH for complete fluorescence quenching (For details see Appendix).

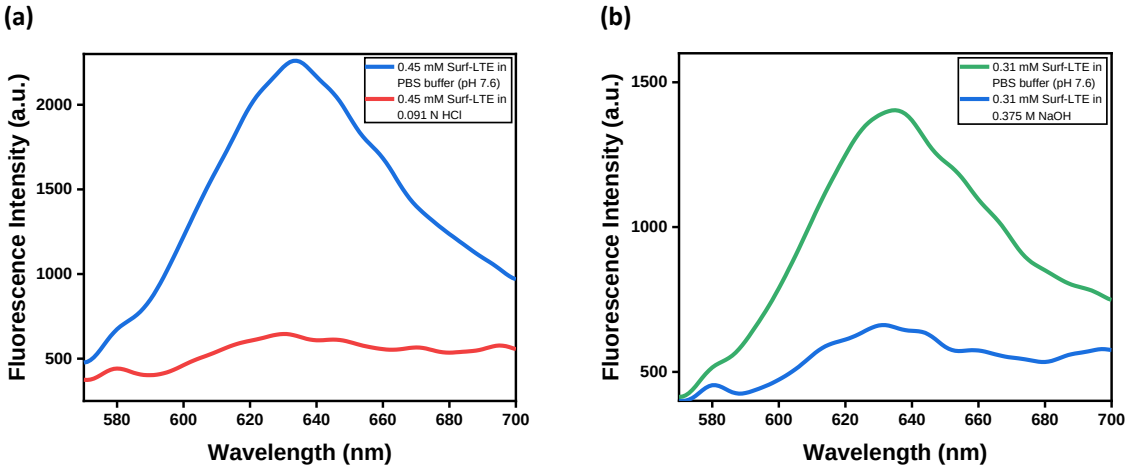

Figure 3.15. Plots representing fluorescence quenching of NR-Surf-LTE complex in presence of (a) HCl and (b) NaOH. Starting concentration of the aqueous solution is 0.5 mM with respect to Surf-LTE.

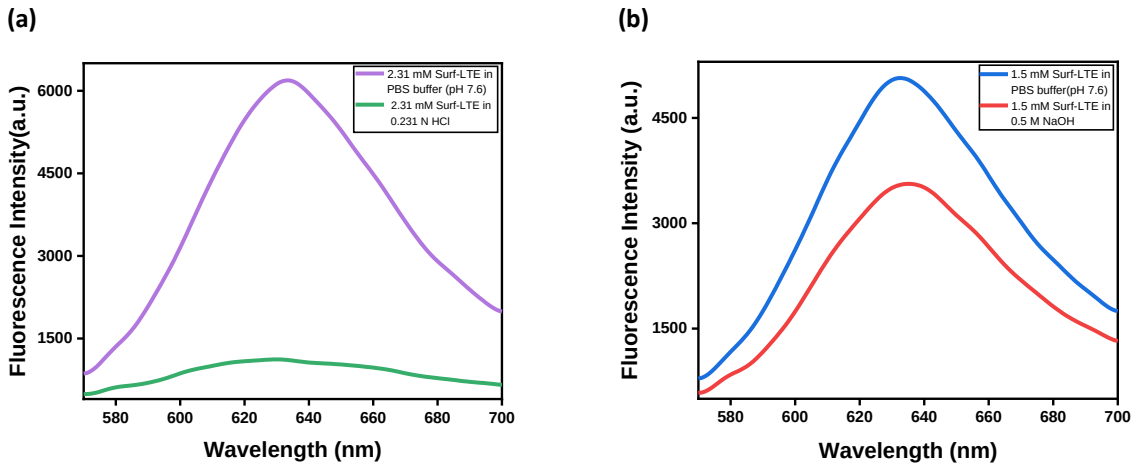

Figure 3.16. Plots representing fluorescence quenching of NR-Surf-LTE complex in presence of (a) HCl and (b) NaOH. Starting concentration of the aqueous solution is 3 mM with respect to Surf-LTE.

b) Lipase action on Surf-LTE

Next, we performed similar experiments using lipase to study its enzymatic action on ester hydrolysis of Surf-LTE. We believe the addition of lipase resulted in a similar breakdown of the micellar structure. Thus the intensity of fluorescence emission gradually decreased. We observed such fluorescence quenching for both 0.5 mM and 3 mM aqueous solutions of Surf-LTE when we added a series of different lipase solutions varying in concentration (1, 2, 5, 10 and 15 μM).

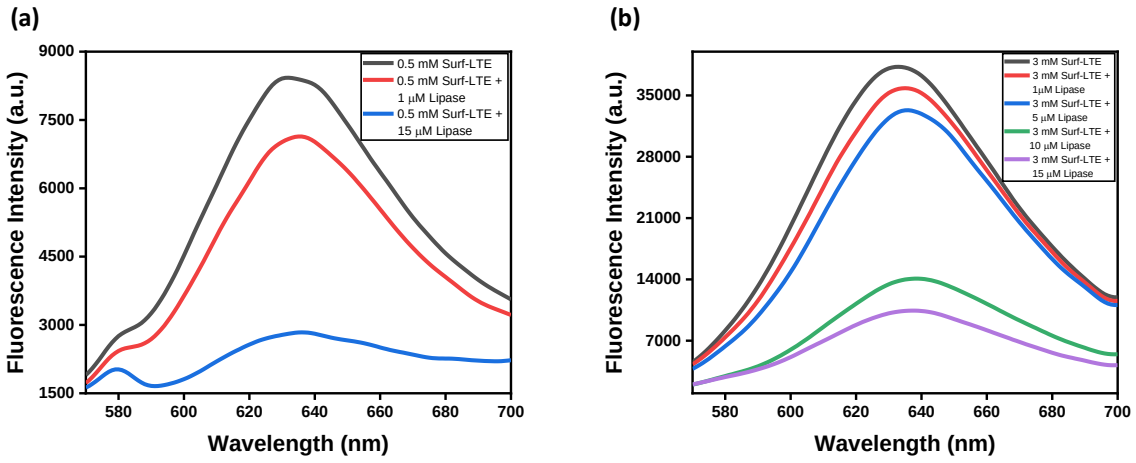

Figure 3.17. Plots representing fluorescence quenching of NR-Surf-LTE complex in presence of lipase; Starting concentration of the aqueous solution is (a) 0.5 mM and (b) 3 mM with respect to Surf-LTE.

Chapter 4

Conclusions

In this work so far, we have demonstrated a straightforward and broad approach to the rational design of nonionic surfactant systems that can be used to program stimuli-responsiveness into nematic LC-aqueous interfaces. We specifically report a laboratory-based synthetic nonionic surfactant, Surf-LTE, which responds to the enzymatic activity of lipase by undergoing ester hydrolysis. We have performed a series of polarized optical microscopy (POM) investigations and fluorescence spectroscopic measurements to support our claim.

First, we have measured the critical micelle concentration (CMC) of Surf-LTE using DPH assay (fluorescence probe method). The CMC was found to be 3.28 mM. Thus we have performed all of our POM measurements at concentrations much lower than 3.28 mM to avoid solubilization of LC mesogens inside the micelle.

Next, we found that both Surf-LTE and lauric acid when adsorbed at the aqueous-LC interface (with an areal density greater than the critical value) induce planar to homeotropic anchoring transition of the LC mesogens, resulting in a macroscopic dark optical output. The hydrophobic interaction between the tails of both molecules with LC mesogens imparted homeotropic anchoring.

We also found that variation of pH and salt concentration did not induce any change in the homeotropic anchoring of Surf-LTE. The results are in good agreement with the past reports. [32-34] Nonionic surfactants are insensitive to the variation of ionic strength of the medium, also the extremely stable structure of the PEG mono ester surfactant is independent of the mild pH variation conditions. Whereas, changing the pH from acidic to basic did impart a change in the orientational anchoring of LC mesogens when lauric acid

molecules were adsorbed at the interface. With increasing pH lauric acid molecules separate from blk LCs and adsorb at aqueous-LC interfaces which is followed by desorption of laurate ions from the aqueous interface into the bulk aqueous medium, resulting in the corresponding optical signal by inducing changes in the anchoring of LC mesogens.

Upon studying the enzymatic activity of lipase on Surf-LTE, we observed a change in the optical signal from dark to bright. Lipase hydrolyses the ester bond present in the surfactant molecules and cleaves Surf-LTE into lauric acid and tetra ethylene glycol chains. We quantified this phenomenon in case of 0.5 wt% Surf-LTE doped LC systems using average grayscale intensity vs. time plot; we found that with increasing concentration of lipase in the bulk medium, the rate of hydrolysis increased. Similar results were also observed when we incubated an aqueous solution of 0.5 mM Surf-LTE with different concentrations of lipase. Thus we obtained similar results from both precelaved moieties and cleaved Surf-LTE moieties upon observing using the crossed polars of the polarized optical microscope.

Lastly, we checked the nonspecific binding interactions of the protein bovine serum albumin (BSA) with Surf-LTE and lauric acid at the aqueous-LC interface. We observed no change in the optical signal of Surf-LTE doped LC system in presence of BSA, while lauric acid doped system gave a transition from dark to bright in the optical response under the crossed polars. The results verify the fact that polyethylene glycol (PEG) decorated surfaces mask the non-specific interactions of BSA, while there is hydrophobic interactions present between the protein and lauric acid molecules. Thus we obtain a change from dark to bright optical appearance for lauric acid doped LC systems upon addition of BSA.

In summary, our results so far describe a synthetic cleavable nonionic surfactant that responds to a broad range of environmental stimuli and can be used as responsive nonionic surfactants in smart LC materials. This is a label-free method that can detect biomolecular events at the interface over time without the use of complex instruments. We also believe that our approach in this work can facilitate the application of stimuli-responsive LCs in the field of drug delivery thus enhancing its potential in the advancement of therapeutics.

Bibliography

1. Collings, P. J. *Liquid Crystals: Nature's Delicate Phase of Matter*. Princeton University Press, **2002**.
2. Collings, P. J.; Goodby, J. W. *Introduction to Liquid Crystals: Chemistry and Physics*. CRC Press, **2019**.
3. Reinitzer, F. Contributions to the knowledge of cholesterol. *Liq. Cryst.* **1989**, *5*, 7-18.
4. Lehmann, O. Über fliessende krystalle. *Zeitschrift für physikalische Chemie* **1889**, *4*, 462-472.
5. An, J.-G.; Hina, S.; Yang, Y.; Xue, M.; Liu, Y. CHARACTERIZATION OF LIQUID CRYSTALS: A LITERATURE REVIEW. *Rev. Adv. Mater. Sci.* **2016**, *44*, 398-406.
6. Dingemans, T. J., Madsen, L. A.; Zafiropoulos, N.A; Lin, W.; Samulski, E.T. Uniaxial and biaxial nematic liquid crystals. *Philosophical Transactions of the Royal Society A: Mathematical, Physical and Engineering Sciences* **2006**, *364*, 2681-2696.
7. Villada-Gil, S.; Palacio-Betancur, V.; Armas-Pérez, J. C.; de Pablo, J. J; Hernández-Ortiz, J. P. Fluctuations and phase transitions of uniaxial and biaxial liquid crystals using a theoretically informed Monte Carlo and a Landau free energy density. *J. Phys.: Condens. Matter* **2019**, *31*, 175101.
8. Carlton, R. J.; Gupta, J. K.; Swift, C. L.; Abbott, N. L. Influence of Simple Electrolytes on the Orientational Ordering of Thermotropic Liquid Crystals at Aqueous Interfaces. *Langmuir* **2012**, *28*, 31-36.
9. Bai, Y.; Abbott, N. L. Recent advances in colloidal and interfacial phenomena involving liquid crystals. *Langmuir* **2011**, *27*, 5719-5738.
10. Popov, P.; Mann, E. K.; Jákli, A. Thermotropic liquid crystal films for biosensors and beyond. *J. Mater Chem. B* **2017**, *5*, 5061-5078.
11. Brake, J. M.; Abbott, N. L. An Experimental System for Imaging the Reversible Adsorption of Amphiphiles at Aqueous− Liquid Crystal Interfaces. *Langmuir* **2002**, *18*, 6101-6109.
12. Brake, J. M.; Daschner, M. K.; Luk, Y.-Y.; Abbott, N. L. Biomolecular Interactions at Phospholipid-Decorated Surfaces of Liquid Crystals. *Science* **2003**, *302*, 2094-2097.
13. Dave, N.; Joshi, T. A Concise Review on Surfactants and its Significance. *Int. J. Appl. Chem* **2017**, *13*, 663-672.

14. Schramm, L. L., Stasiuk, E. N.; Marangoni, D. G. 2 Surfactants and their applications. *Annu. Rep. Prog. Chem., Sect. C: Phys. Chem.* **2003**, *99*, 3-48.
15. Halliday, H. L. The fascinating story of surfactant. *J. Paediatr. Child Health* **2017**, *53*, 327-332.
16. Schmitt, T. M. Analysis of Surfactants. CRC Press, **2001**.
17. Rosen, M. J.; Kunjappu, J. T. Surfactants and Interfacial Phenomena. John Wiley & Sons, **2012**.
18. Schick, M. J., ed, Dekker, M. Nonionic Surfactants: Physical Chemistry. CRC Press, **1987**.
19. Fletcher, P. D. I.; Kang, N.-G.; Paunov, V. N. UV Polymerisation of Surfactants Adsorbed at the Nematic Liquid Crystal–Water Interface Produces an Optical Response. *ChemPhysChem* **2009**, *10*, 3046-3053.
20. Gupta, V. K.; N. L. Abbott. Design of Surfaces for Patterned Alignment of Liquid Crystals on Planar and Curved Substrates. *Science* **1997**, *276*, 1533-1536.
21. Gupta, V. K., Skaife, J. J.; Dubrovsky, T. B.; Abbott, N. L. Optical Amplification of Ligand-Receptor Binding using Liquid Crystals. *Science* **1998**, *279*, 2077-2080.
22. Shah, R. R.; Abbott, N. L. Using Liquid Crystals To Image Reactants and Products of Acid−Base Reactions on Surfaces with Micrometer Resolution. *J. Am. Chem. Soc.* **1999**, *121*, 11300-11310.
23. Skaife, J. J.; Abbott, N. L. Quantitative Interpretation of the Optical Textures of Liquid Crystals Caused by Specific Binding of Immunoglobulins to Surface-Bound Antigens. *Langmuir* **2000**, *16*, 3529-3536.
24. Lee, B.-w.; Clark, N. A. Alignment of Liquid Crystals with Patterned Isotropic Surfaces. *Science* **2001**, *291*, 2576-2580.
25. Hoogboom, J.; Velonia, K.; Rasing, T.; Rowan, A. E.; Nolte, R. J. M. LCD-based detection of enzymatic action. *Chem. Commun.* **2006**, 434-435.
26. Tingey, M. L.; Wilyana, S.; Snodgrass, E. J.; Abbott, N. L. Imaging of Affinity Microcontact Printed Proteins by Using Liquid Crystals. *Langmuir* **2004**, *20*, 6818-6826.
27. Lockwood, N. A.; Abbott, N. L. Self-assembly of surfactants and phospholipids at interfaces between aqueous phases and thermotropic liquid crystals. *Current Opin. Colloid Interface Sci.* **2005**, *10*, 111-120.

28. Park, J.-S.; Teren, S.; Tepp, W. H.; Beebe, D. J.; Johnson, E. A.; Abbott, N. L. Formation of Oligopeptide-Based Polymeric Membranes at Interfaces between Aqueous Phases and Thermotropic Liquid Crystals. *Chem. Mater.* **2006**, *18*, 6147.
29. Clare, B. H.; Efimenko, K.; Fischer, D. A.; Genzer, J.; Abbott, N. L. Orientations of Liquid Crystals in Contact with Surfaces that Present Continuous Gradients of Chemical Functionality. *Chem. Mater.* **2006**, *18*, 2357-2363.
30. Clare, B. H.; Guzmán, O.; de Pablo, J. J.; Abbott, N. L. Measurement of the Azimuthal Anchoring Energy of Liquid Crystals in Contact with Oligo(ethylene glycol)-Terminated Self-Assembled Monolayers Supported on Obliquely Deposited Gold Films. *Langmuir* **2006**, *22*, 4654-4659.
31. Tjipto, E.; Cadwell, K. D.; Quinn, J. F.; Johnston, A. P. R.; Abbott, N. L.; Caruso, F. Tailoring the Interfaces between Nematic Liquid Crystal Emulsions and Aqueous Phases via Layer-by-Layer Assembly. Nano Lett. **2006**, *6*, 2243-2248.
32. Lockwood, N. A.; de Pablo, J. J.; Abbott, N. L. Influence of Surfactant Tail Branching and Organization on the Orientation of Liquid Crystals at Aqueous−Liquid Crystal Interfaces. *Langmuir* **2005**, *21*, 6805-6814.
33. Brake, J. M.; Mezera, A. D.; Abbott, N. L. Effect of Surfactant Structure on the Orientation of Liquid Crystals at Aqueous−Liquid Crystal Interfaces. *Langmuir* **2003**, *19*, 6436-6442.
34. Brake, J. M.; Abbott, N. L. An Experimental System for Imaging the Reversible Adsorption of Amphiphiles at Aqueous−Liquid Crystal Interfaces. *Langmuir* **2002**, 18, 6101-6109.
35. Kim, Y.-K.; Huang, Y.; Tsuei, M.; Wang, X.; Gianneschi, N. C.; Abbott, N. L. Multi-Scale Responses of Liquid Crystals Triggered by Interfacial Assemblies of Cleavable Homopolymers. *ChemPhysChem* **2018**, *19*, 2037-2045.
36. Kim, Y.-K.; Raghupathi, K. R.; Pendery, J. S.; Khomein, P.; Sridhar, U.; de Pablo, J. J.; Thayumanavan, S.; Abbott, N. L. Oligomers as Triggers for Responsive Liquid Crystals. *Langmuir* **2018**, *34*, 10092-10101.
37. Stjerndahl, M.; Holmberg, K. Synthesis and chemical hydrolysis of surface-active esters. *J Surfact Deterg* **2003**, *6*, 311-318.
38. Li, W.; Sun, J.; Zhang, X.; Jia, L.; Qiao, M.; Zhao, X.; Hu, H.; Chen, D.; Wang, Y. Synthesis and Characterization of pH-responsive PEG-poly (β-amino ester) Block Copolymer Micelles as Drug Carriers to Eliminate Cancer Stem Cells. *Pharmaceutics* **2020**, *12*, 111.

39. Suk, J. S.; Xu, Q.; Kim, N.; Hanes, J.; Ensign, L. M. PEGylation as a Strategy for Improving Nanoparticle-Based Drug and Gene Delivery. *Adv. Drug Deliv. Rev.* **2016**, *99*, 28-51.
40. Wu, J.; Xie, X.; Zheng, Z.; Li, G.; Wang, X.; Y. Wang. Effect of pH on polyethylene glycol (PEG)-induced silk microsphere formation for drug delivery. *Mater. Sci. Eng. C* **2017**, *80*, 549-557.
41. Manson, J.; Kumar, D.; Meenan, B. J.; Dixon, D. Polyethylene glycol functionalized gold nanoparticles: the influence of capping density on stability in various media. *Gold Bull.* **2011**, *44*, 99-105.
42. Kong, L.; Yang, Q.; Xing, H.; Su, B.; Bao, Z.; Zhang, Z.; Yang, Y.; Ren, Q. A general method for the separation of amphiphilic surface-active poly (ethylene glycol) mono- and di-esters with long-chain ionic liquid-based biphasic systems. *Green Chem.* **2014**, *16*, 102-107.
43. Wishnia, A.; Pinder, T. Hydrophobic Interactions in Proteins: Conformation Changes in Bovine Serum Albumin below pH 5. *Biochemistry* **1964**, *3*, 1377-1384.
44. Agarwal, A.; Huang, E.; Palecek, S.; Abbott, N. L. Optically Responsive and Mechanically Tunable Colloid-In-Liquid Crystal Gels that Support Growth of Fibroblasts. *Adv. Mater.* **2008**, *20*, 4804-4809.
45. Brake, J. M.; Abbott, N. L. Coupling of the Orientations of Thermotropic Liquid Crystals to Protein Binding Events at Lipid-Decorated Interfaces. *Langmuir* **2007**, *23*, 8497–8507
46. Fluksman, A.; Benny, O. A robust method for critical micelle concentration determination using coumarin-6 as a fluorescent probe. *Anal. Methods* **2019**, *11*, 3810-3818.
47. Chattopadhyay, A.; London, E. Fluorimetric determination of critical micelle concentration avoiding interference from detergent charge. *Anal. Biochem.* **1984**, *139*, 408-412.
48. Prazeres, T. J. V.; Beija, M.; Fernandes, F. V.; Marcelino, P. G. A.; Farinha, J. P. S.; Martinho, J. M. G. Determination of the critical micelle concentration of surfactants and amphiphilic block copolymers using coumarin 153. *Inorganica Chim. Acta* **2012**, *381*, 181-187.
49. Mehreteab, A.; Chen, B. Fluorescence technique for the determination of low critical micelle concentrations. *J. Am. Oil Chem.' Soc.* **1995**, *72*, 49-52.
50. Zhong, S.; C.-H. Jang. pH-Driven adsorption and desorption of fatty acid at the liquid

crystal–water interface. *Liq. Cryst.* **2016**, *43*, 361-368.

51. Hu, Q.-Z.; Jang, C.-H. Spontaneous formation of micrometer-scale liquid crystal droplet patterns on solid surfaces and their sensing applications. *Soft Matter* **2013**, *9*, 5779-5784.
52. Hu, Q.-Z.; Jang, C.-H. A simple strategy to monitor lipase activity using liquid crystal-based sensors. *Talanta* **2012**, *99*, 36-39.
53. Hendow, S. T. 12 - Optical Materials and Devices. *Experimental Methods in the Physical Sciences* **1997**, *29*, 343-367.
54. Verma, I.; Rajeev, N.; Mohiuddin, G.; Pal, S. K. Ordering Transitions in Liquid Crystals Triggered by Bioactive Cyclic Amphiphiles: Potential Application in Label-Free Detection of Amyloidogenic Peptides. *J. Phys. Chem. C* **2019**, 123, 11, 6526–6536.
55. Wei, H.; Zhuo, R.-X.; Zhang, X.-Z. Design and development of polymeric micelles with cleavable links for intracellular drug delivery. *Prog. Polym. Sci.* **2013**, 38, 503–535.

Appendix

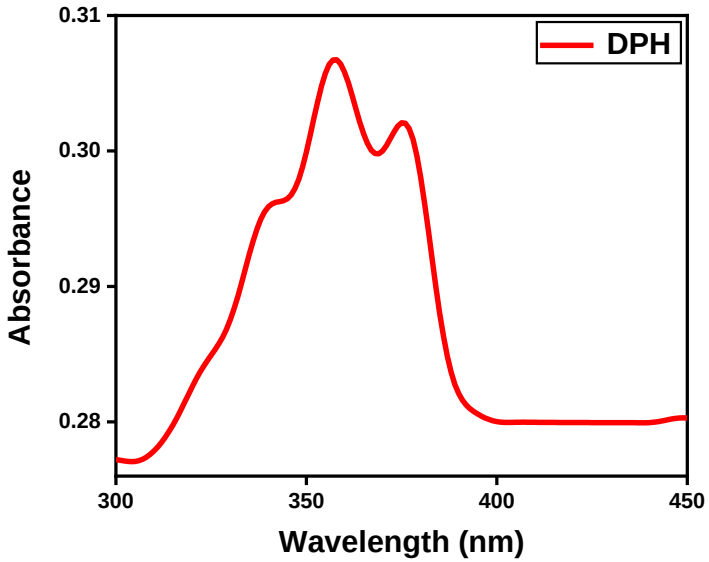

Figure A1. Absorption spectrum of DPH-Surf-LTE complex at pH 7.6.

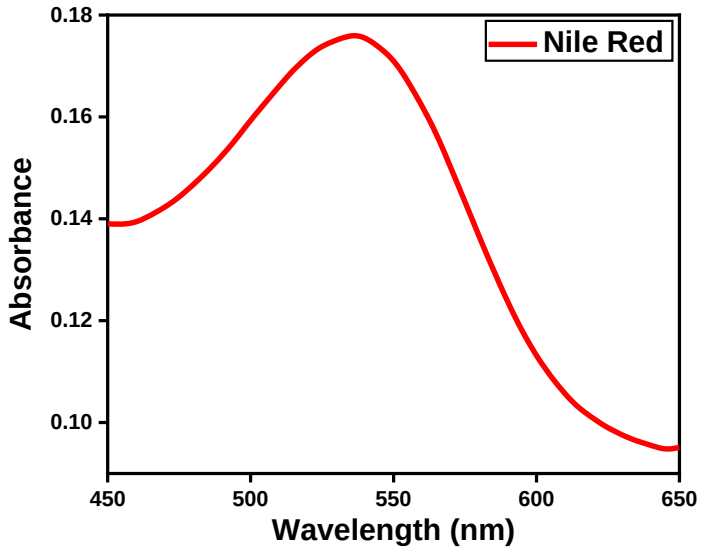

Figure A2. Absorption spectrum of NR-Surf-LTE complex at pH 7.6.

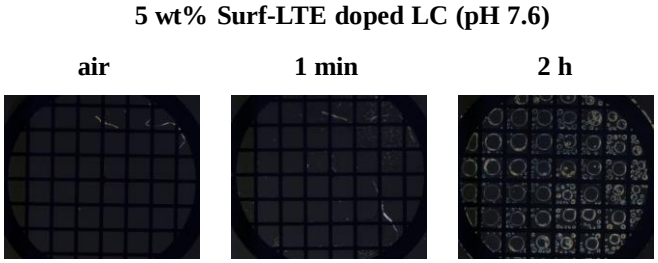

Figure A3. POM images of 5 wt% Surf-LTE doped 5CB film at air-LC interface and aqueous-LC interface (10 mM PBS buffer medium at pH 7.6). Scale bar = 200 μm.

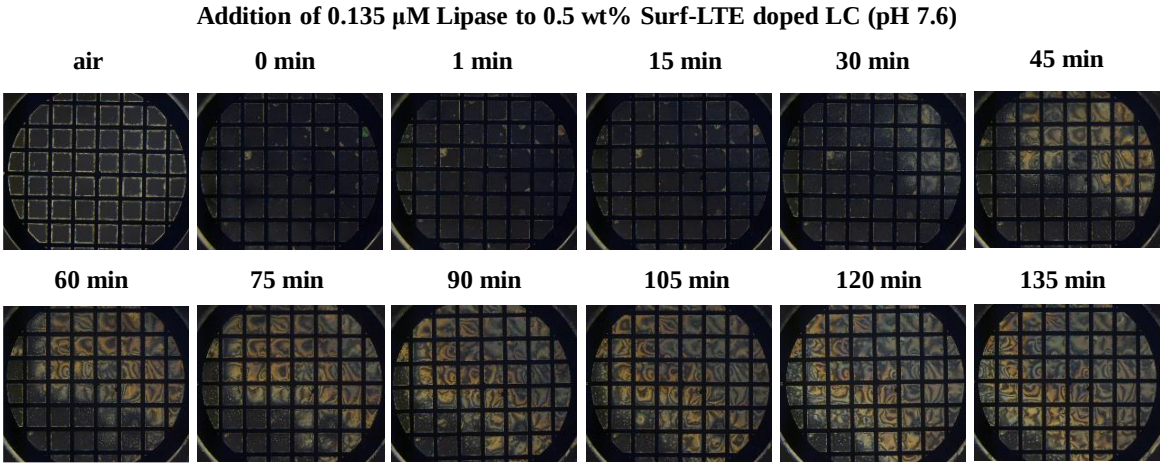

Figure A4. POM images of 0.5 wt% Surf-LTE doped 5CB film at aqueous-LC interface in 10 mM PBS buffer medium (pH 7.6) showing dynamic response of LC due to the presence of 0.135 μM lipase at different time intervals. Scale bar = 200 μm.

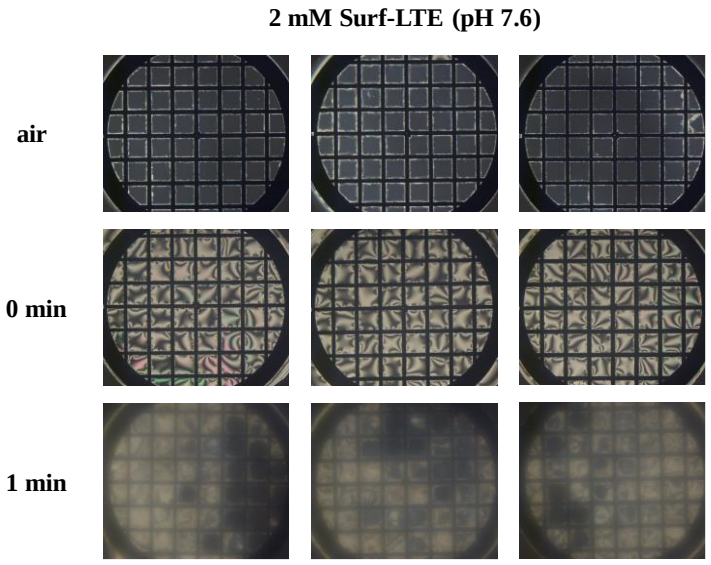

Figure A5. POM images of 5CB film after the introduction of 2 mM aqueous solution of Surf-LTE (at pH 7.6). Scale bar = 200 μm.

Calculation of Doping mixtures (wt%)

Calcuation of 0.01 wt% Surf-LTE/LA doped LC mixture:

Surf-LTE/LA stock solution: 1 mg/ml in $CHCl_3$

Amount of 5CB: 10 μL

Density of 5CB: 1.01 gm/ml

Weight of 5CB: $10\times10^{-3}\times1.01$ gm = 10.1 mg

Therefore, Amount of Surf-LTE/LA = (0.01×10.1)/100 mg

= 0.00101 mg

Therefore Volume of Surf-LTE/LA = 0.00101 mg/(1 mg/ml)

= 0.00101 ml

= 1.01 μL

Similarly, rest of the weight percentages are calculated.

Substrate to enzyme ratio for interfacial ester hydrolysis

Density of 5CB = 1.01 gm/ml

Thus, 0.2 μL 5CB = [(0.2×1.01)/1000] mg

= 0.202 mg

Therefore, amount of Surf-LTE = [(0.5×0.202)/100] mg

= 1.01×10^{-3} mg

Therefore, number of moles of Surf-LTE = (1.01×10^{-6} gm)/(376.53 gm/mol)

= 2.68×10^{-9} mols

= 0.00268 μmols

Molecular weight of Lipase = 33 kDa

= 33×10^{3}

Concentration of Lipase stock = 1 mg/ml ≈ 30.3 μM

Now, Amount of Lipase present per grid = (0.5μM×2 ml)

= (0.0165 mg/ml × 2 ml)

= 0.033 mg

Thus, number of moles of Lipase = 0.033 mg/(33×10^{3} gm/mol)

= 0.001×10^{-6} moles

= 0.001 μmoles

Therefore, substrate to enzyme ratio is given as = 0.00268/0.001

= 2.68:1

Fluorescence Quenching experiments with HCl

Voulme of Surf-LTE (μL)	Concentration of Surf-LTE (mM)	Voulme of HCl (μL)	Concentration of HCl (N)	Total Volume (μL)
200	3	-	-	200
200	2.73	20	0.091	220
200	2.50	40	0.167	240
200	2.31	60	0.231	260

Voulme of Surf-LTE (μL)	Concentration of Surf-LTE (mM)	Voulme of HCl (μL)	Concentration of HCl (N)	Total Volume (μL)
200	0.5	-	-	200
200	0.45	20	0.091	220

Fluorescence Quenching experiments with NaOH

Voulme of Surf-LTE (μL)	Concentration of Surf-LTE (mM)	Voulme of NaOH (μL)	Concentration of NaOH (M)	Total Volume (μL)
200	3	-	-	200
200	2.73	20	0.091	220
200	2.5	40	0.167	240
200	2.31	60	0.231	260
200	2.14	80	0.286	280
200	2	100	0.333	300
200	1.87	120	0.375	320
200	1.76	140	0.412	340
200	1.67	160	0.444	360
200	1.57	180	0.474	380
200	1.5	200	0.5	400

Voulme of Surf-LTE (μL)	Concentration of Surf-LTE (mM)	Voulme of NaOH (μL)	Concentration of NaOH (M)	Total Volume (μL)
200	0.5	-	-	200
200	0.45	20	0.091	220
200	0.42	40	0.167	240
200	0.38	60	0.231	260
200	0.36	80	0.286	280
200	0.33	100	0.333	300
200	0.31	120	0.375	320